

WINNET: TIME SERIES FORECASTING WITH A WINDOW-ENHANCED PERIOD EXTRACTING AND INTERACTING

Anonymous authors

Paper under double-blind review

ABSTRACT

Recently, Transformer-based methods have significantly improved state-of-the-art time series forecasting results, but they suffer from high computational costs and the inability to capture the long and short periodicity of time series. We present a highly accurate and simply structured CNN-based model for long-term time series forecasting tasks, called WinNet, including (i) Inter-Intra Period Encoder (I2PE) to transform 1D sequence into 2D tensor with long and short periodicity according to the predefined periodic window, (ii) Two-Dimensional Period Decomposition (TDPD) to model period-trend and oscillation terms, and (iii) Decomposition Correlation Block (DCB) to leverage the correlation of the period-trend and oscillation terms to support the prediction tasks by CNNs. Results on nine benchmark datasets show that the WinNet can achieve SOTA performance and lower computational complexity over CNN-, MLP-, Transformer-based approaches. The WinNet provides potential for the CNN-based methods in the time series forecasting tasks, with perfect tradeoff between performance and efficiency.

1 INTRODUCTION

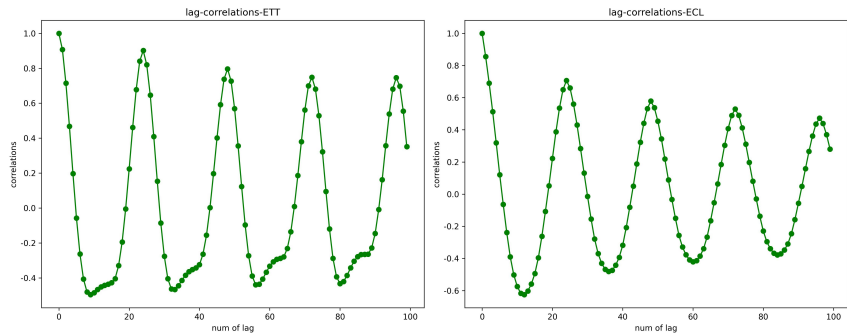
Time series forecasting (TSF) has been widely used in the prediction of energy consumption, transportation, economic planning, weather and disease transmission. The TSF tasks are to leverage the known sequence of multiple time steps to predict the information of multiple time steps in the future, which further facilitates resource planning and management. Extensive neural architectures have been designed to achieve the TSF tasks. Recent deep learning models have achieved significant performance improvements, such as Informer (Zhou et al., 2021), AutoFormer (Wu et al., 2021), FEDformer (Zhou et al., 2022), DLinear (Zeng et al., 2023), TimesNet (Wu et al., 2023), PatchTST (Nie et al., 2023). Benefiting from the self-attention mechanism, the Transformer-based models are able to capture the long-term dependency of temporal sequence, achieving state-of-the-art (SOTA) performance for TSF tasks. However, these models are not sensitive to the periodicity and have high computational complexity. Recently, the DLinear outperforms the Transformer-based architectures with only a single linear layer, which results in increasing research attentions and discussions between the MLP-based and the Transformer-based architectures. In the TimesNet, the classical convolutional neural network (CNN) is applied to extract the periodic features after converting the sequence into two-dimensional (2D) tensor by multi-periods, which also inspires us to reconsider the CNN-based methods in the TSF tasks.

Since the future status of a system is time-evolving and with uncertainties, the TSF tasks can be quite challenging. Except for the temporal and regular changes, the uncertainties of the time series data, as well as the noise inputs, provide extra technical difficulties to apply the trend and seasonal terms to achieve the TSF tasks. However, the performance of the model is strongly correlated with the periodicity. A new method of setting up a periodic window is proposed to process the multi-periods of the time series and the corresponding neural network model is designed to capture the complicated underlying patterns of temporal sequence. The network mainly extracts periodicity of the time series through the periodic **window**, called WinNet.

In the WinNet, the original sequence is transformed by MLP layer to extract the periodicity. The periodic window is approximated as the least common multiple of multi-periods obtained by the Fast Fourier Transformation (FFT) (Wu et al., 2023). In this way, the periodic window can represent the variation of multiple short periods, and the sequence is organized into 2D tensor according to the

periodic window. In the 2D tensor, each row represents the short-period trend within the periodic window, and each column represents the long-period trend of the whole sequence. Subsequently, the features of long and short periods are separately extracted by the I2PE. The TDPD module is proposed to decompose the 2D tensor into the period-trend and oscillation terms, which highlights the importance of periodicity. **Based on the correlation analysis, we find that there are extremely strong lag-correlations between the trend and seasonal terms, and the correlation has a periodic pattern, as shown in Figure 1.** To mine their correlation instead of utilizing them separately like DLinear and MICN, the DCB is innovatively designed to combine the period-trend and oscillation terms using a convolutional kernel. The learned weights of the convolution kernel represent the importance of the period-trend and oscillation terms of neighboring time steps. To perform an efficient periodic fusion of the time series, the Series Decoder is proposed to interactively combine the features of long and short period and map the learned features into the prediction of time steps. The WinNet can reduce the relative Mean Squared Error (MSE) and Mean Absolute Error (MAE) in multivariate time series by 18.5% and 12.0%, respectively, compared to TimesNet.

Figure 1: The lag correlations of the trend and seasonal terms in ETTm1 and ECL datasets. We can see that the lag-correlations between the two terms are very strong and there is a periodic pattern.



In summary, this work contributes the time series forecasting tasks in the following ways:

- Only one convolutional layer is designed as the backbone of the prediction network, which greatly reduces the training memory and computational complexity and improves experimental efficiency. This also indicates that the simple model architecture can also be effective for the TSF tasks.
- The time series are reorganized according to a periodic window, which can represent the trend variation of multiple short periods.
- To enhance the modeling ability, time series are further decomposed into the period-trend and oscillation terms by the TDPD module. The DCB is proposed to aggregate the neighboring periodic information to obtain the local periodicity by extracting the correlation between the two terms.
- Extensive experiments are conducted on 9 benchmark datasets across multiple domains (energy, traffic, economics, weather, electricity and illness). Our experimental results demonstrate that the WinNet outperforms other comparative baselines in both the univariate and multivariate prediction tasks with long and short input lengths. The WinNet provides potential for the CNN-based methods in the TSF tasks.

2 RELATED WORK

It is widely recognized that the uncertainties of the temporal sequence provide extra difficulties in the TSF tasks. In recent years, extensive deep learning models have been proposed to achieve the temporal modeling, including RNN-based, CNN-based, Transformer-based, and MLP-based models. The SOTA performance and specific advantages are demonstrated by extensive experiments, as shown below:

RNNs In general, RNN networks are the primary tools for temporal modeling before the Transformer architecture. RNN-based methods, such as LSTM (Hochreiter & Schmidhuber, 1997), GRU (Chung et al., 2014) and DeepAR (Salinas et al., 2020), utilize the recurrent information transmission to capture the temporal changes through state transitions among time steps.

Transformers Transformer (Vaswani et al., 2017) and its variants are also initially proposed to achieve the Natural Language Processing tasks, with the advantage of parallel recurrent computation and the self-attention mechanism to capture the long-term temporal correlation. Currently Transformer has been widely used in TSF tasks, such as the Informer, Autoformer, FEDformer, Crossformer (Zhang & Yan, 2023), PatchTST, PETformer (Lin et al., 2023), etc. The attention mechanism is designed to capture the temporal dependencies among time steps and achieve significant performance in the TSF tasks. In the Autoformer, the sequence trend decomposition is to capture the temporal pattern of a sequence by the trend and seasonal terms, and an auto-correlation mechanism is to capture the temporal dependence of the series based on learning periods. In the FEDformer, a Fourier enhanced structure is designed to enhance sparse attention in the frequency domain. By referring to the Vision Transformer (Dosovitskiy et al., 2020), the PatchTST utilizes the slice and dice strategy to formulate the patch and the Transformer architecture is applied to extract local semantic information of the multivariate time series.

MLPs DLinear has been proven to be effective for TSF, which achieve competitive performance over the Transformer architecture by a simple one-layer linear transformation with channel independence (CI). Since then, many MLP-based models are proposed to encode temporal dependencies for the TSF tasks, including LightTS (Zhang et al., 2022), MTS-Mixers (Li et al., 2023b), TSMixer (Ekambaram et al., 2023), RLinear (Li et al., 2023a), etc. The MLP-based methods significantly address the computational efficiency issue of Transformer, and their simplified model structures allow them to be another prominent architecture for TSF tasks.

CNNs CNN networks were mainly used in the field of Computer Vision, where they can be used to extract local information from images. Recently, CNNs have been proposed to mine the periodicity of time series, such as TCN (Bai et al., 2018), TimesNet, MICN, etc. The TCN captures temporal changes through a convolutional kernel that slides along the temporal dimension. In the TimesNet, the original sequence is reshaped into the 2D tensor by periods to extract multiple periods of the sequence by FFT. The classical InceptionV1 network (Szegedy et al., 2015) is applied to process the temporal samples within the periods to support the forecasting tasks. A multi-scale isometric convolutional network with multi-scale branches is proposed in the MICN to capture both local and global features from a holistic view of the temporal sequence.

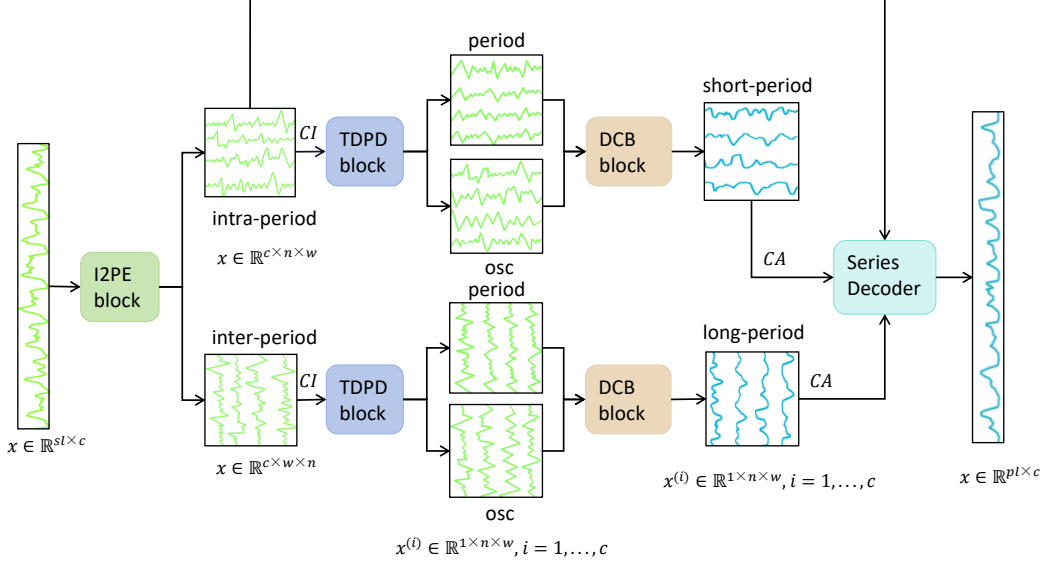
3 WINNET

The general architecture of WinNet is illustrated in Figure 2. As mentioned before, based on the multi-periodic features of time series, the periodic window with the superposition of multiple periods is proposed to capture the periodic changes of the time series within the periodic window. I2PE block is designed to extract the periodicity of the sequence and obtain intra-period and its transpose (inter-period). The intra-period indicates that the rows of the 2D tensor are the periodic windows, while the inter-period indicates that the columns are the periodic windows. The TDPD is separately performed on the two features to obtain the period-trend and oscillation terms. The DCB is followed to learn the local correlation between the period-trend and oscillation terms, respectively. The final prediction results are obtained by the Series Decoder.

3.1 INTER-INTRA PERIOD ENCODER

In DLinear, a single linear layer has the ability to effectively capture periodicity in the time series. We perform a linear layer on the original sequence (Li et al., 2023b), and the linear mapped sequence can acquire the periodic information from each sample in the original sequence. We find that the MLP layer can reduce the period of the original sequence dramatically, making the period characteristics more obvious and facilitating the period extraction for CNN network. For the top-k periods obtained by FFT in Appendix Table 8, multiple short periods are encapsulated within the periodic window, facilitating the extraction of multiple short periods using the convolutional networks for

Figure 2: The model architecture of WinNet. The period and osc represent the period-trend and oscillation terms. CI and CA mean the channel independence and aggregation strategy, similar to DLinear(Zeng et al., 2023), and sl, pl indicate the input and prediction length. c, n, w represent the number of channel, periodic window and the periodic window size, respectively. The output (in blue) is the final result of the TSF tasks.



complex sequences. As shown in Appendix Figure 8, the periodic window is approximated as the least common multiple of each refined period.

After the operations in I2PE block, the original sequence is reshaped into a 2D tensor according to the size of the periodic window, as shown in the [equation 1](#):

$$\begin{aligned}
 \hat{\mathbf{X}}_{1D} &= \text{Permute}(\text{RevIN}(\mathbf{X}_{1D})) \\
 \mathbf{X}_{2D}^{row} &= \text{Reshape}(\text{Linear}(\hat{\mathbf{X}}_{1D})) \\
 \mathbf{X}_{2D}^{col} &= \text{Transpose}(\mathbf{X}_{2D}^{row})
 \end{aligned} \tag{1}$$

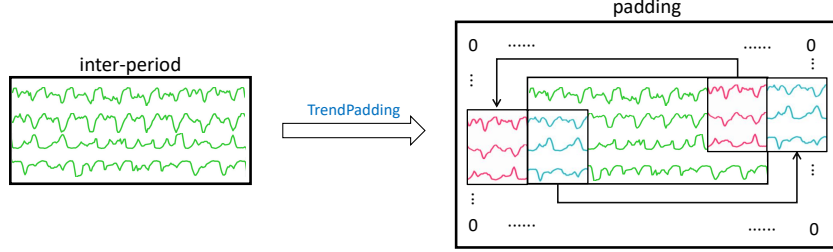
where $\mathbf{X}_{1D} \in \mathbb{R}^{sl \times c}$ is the original sequence, $\mathbf{X}_{2D}^{row} \in \mathbb{R}^{c \times n \times w}$ is the intra-period whose rows represent the periodic windows, while $\mathbf{X}_{2D}^{col} \in \mathbb{R}^{c \times w \times n}$ represents its columns are the periodic windows. The sl and c denote the input length and the number of channels in the sequence, and the n, w are the number of periodic windows and the periodic window size (in the experiments, $n = w$). [RevIN's regularization method is referenced from NLinear \(Zeng et al., 2023\)](#).

Specifically, each row in the intra-period represents a periodic window with the superposition of multiple short periods, and multiple windows are organized into each column to capture the variation of the time series among periodic windows. Since the periodic window size is approximated as a common multiple of the top-k periods of the sequence, the long-periodicity correlation can be found among the column at the corresponding positions in both periodic windows.

3.2 TWO-DIMENSIONAL PERIOD DECOMPOSITION

In general, existing methods for time series trend decomposition mainly focused on trend decomposition of 1D sequence. In this work, inspired by the trend decomposition idea in DLinear, we propose a TDPD strategy, as shown in equation 2. Specifically, a trend-padding operation is dedicatedly designed to perform the convolutional operation at the boundary. As shown in Figure 4, after the operation, the 2D tensor $\mathbf{X}_{2D} \in \mathbb{R}^{s \times n \times w}$ are padded into a new 2D tensor $\mathbf{X}_{2D} \in \mathbb{R}^{s \times (n+p) \times (w+p)}$ where p means the padding lengths in row or column.

Figure 3: The figure of TrendPadding. Unlike the 0 or same padding mode in common CNNs, the neighbor samples (before or after) in the original sequence are selected as the padding item to retain the trend characteristics of the whole sequence. To keep the shape of the matrix, we complement the remaining positions with 0.



$$\begin{aligned} \mathbf{X}_{period} &= \text{AvgPool2D}(\text{TrendPadding}(\mathbf{X}_{2D}))_{k \times k} \\ \mathbf{X}_{osc} &= \mathbf{X} - \mathbf{X}_{period} \end{aligned} \quad (2)$$

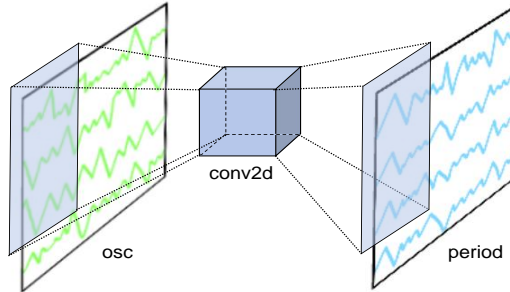
where \mathbf{X}_{period} and \mathbf{X}_{osc} indicate the period-trend and oscillation terms, respectively, and $k \times k$ is the size of the $\text{Avgpool2D}(\cdot)$ kernel size.

Common $\text{Avgpool1D}(\cdot)$ operation focuses on the average change in the trend of time series, while $\text{Avgpool2D}(\cdot)$ is applied to extract both the trend within the periodic window (intra-correlation) and the changes of the long period among the neighbouring windows (inter-correlation). According to the equation 2, the two features can be decomposed into the period-trend and oscillation terms. Specifically, the period-trend term keeps a balance between intra-correlation trends and inter-correlation periodicity. As shown in Appendix Figure 7, we can see that the trend of the time steps among each window keeps essentially the same.

3.3 DECOMPOSITION CORRELATION BLOCK

After decomposing the sequence into the trend and seasonal terms, DLinear simply feeds the trend and seasonal terms independently into a linear layer for model training. MICN predicts the seasonal term by the proposed MIC layer, while the trend-cyclical part is directly obtained by linear regression. They fail to capture the correlation between trend and seasonal terms.

Figure 4: The figure of DCB. The period and osc represent the period-trend and oscillation terms. Use a convolutional kernel to extract the variation of the two terms within the periodic neighborhood.



We believe that there is a correlation between period-trend and oscillation terms and that they are influencing future time steps together. Specifically, time steps in the sequence can be affected by the period-trend and oscillation terms obtained by TDPD within the moments of periodic neighborhood. The CNN kernel can exactly extract the variation of the two terms within periodic neighborhood, and the learned parameters are able to perform a proportional aggregation of them, instead of simply adding. We choose CNN as our backbone network to synthesize the sequence information of N

time steps in the periodic neighborhood. The process is described below:

$$\begin{aligned}
\mathbf{X}_{period}^{CI}, \mathbf{X}_{osc}^{CI} &= \text{CI}(\mathbf{X}_{period}), \text{CI}(\mathbf{X}_{osc}) \\
\mathbf{X}_{input}^{CI} &= \text{Concat}(\mathbf{X}_{period}^{CI}, \mathbf{X}_{osc}^{CI}) \\
\hat{\mathbf{X}}_{output}^{CI} &= \text{Dropout}(\text{Sigmoid}(\text{Conv2D}(\mathbf{X}_{input}^{CI}))) \\
\hat{\mathbf{X}}_{output}^{CI} &= \text{CA}(\hat{\mathbf{X}}_{output}^{CI})
\end{aligned} \tag{3}$$

where $\text{CI}(\cdot)$ and $\text{CA}(\cdot)$ mean channel independence and aggregation strategy. In the $\text{CI}(\cdot)$, we split both period-trend and oscillation terms at the channel dimension and concatenate them into two-channel matrices. We feed the matrices at the same channel into the DCB block. In the $\text{CA}(\cdot)$, we concatenate the single-channel output after the DCB block at the channel dimension for fusion.

3.4 SERIES DECODER

The DCB can learn the local correlative features of the time series, and in this section, the Series Decoder is designed to aggregate the inter-period and intra-period for extracting global periodicity of each window. Specifically, the process is:

$$\begin{aligned}
\hat{\mathbf{X}}_{i,j}^{fusion} &= \hat{\mathbf{X}}_{i,j}^{row} + \hat{\mathbf{X}}_{j,i}^{col}, i, j \in (1, 2, \dots, w) \\
\hat{\mathbf{X}}_{i,j}^{res} &= \hat{\mathbf{X}}_{i,j} + \mathbf{X}_{i,j}^{row} \\
\hat{\mathbf{X}}_{i,j}^{final} &= \text{Permute}(\text{Linear}(\text{Reshape}(\hat{\mathbf{X}}_{2D}^{res})))
\end{aligned} \tag{4}$$

where i, j together denote a temporal point of the 2D tensor, w represents the size of the periodic window, matrix $\hat{\mathbf{X}}_{i,j}^{res}$ and $\hat{\mathbf{X}}_{i,j}^{final}$ are the output of residual connection and the final result.

$\mathbf{X}_{i,j}^{row}$ is obtained by intra-period convolution, reflecting the short periodicity of the sequence, and $\mathbf{X}_{j,i}^{col}$ is obtained by inter-period convolution, which is spaced by window size and reflects the long periodicity of the sequence. This design is able to interactively learn the correlation of the short-period time steps with the fusion of the long-period features, thus further extracting the global periodicity of the sequence. After the operation, a simple linear layer is designed to map the learned features into the prediction of time steps.

4 EXPERIMENT

Datasets In this section, a total of 9 real-world datasets¹ are applied to validate the proposed approaches and selective baselines, including weather, traffic, ECL, ILI, exchange and ETT datasets (ETTh1, ETTh2, ETTm1, ETTm2). It should be noted that ETTh1, ETTh2 and ILI are small datasets with small channels, ETTm1, ETTm1 and weather are medium datasets with small channels, and ECL, traffic are large datasets with multi-channels. In general, periodicity is more easily captured for small datasets and more difficult for large datasets.

Baselines and metrics The following methods are selected as the baselines, including Transformer-based PatchTST, Crossformer, FEDformer, Autoformer, CNN-based TimesNet and MICN, and MLP-based DLinear, RLinear and RMLP. All models follow the same experimental setup with a prediction length of $T \in \{24, 36, 48, 60\}$ for the ILI dataset and $T \in \{96, 192, 336, 720\}$ for the other datasets. We collect baseline results from DLinear, PatchTST and TimesNet. The default input length $L=96$ is for the Transformer-based model and $L=512$ is for PatchTST/64. To ensure the effectiveness of the Transformer and DLinear-based methods, two input lengths $\{96$ and $512\}$, are applied to conduct the performance comparison with SOTA models. In addition, we also explore the influence of the size of the input length on the performance of the proposed model. The Mean Squared Error (MSE) and Mean Absolute Error (MAE) are selected to measure the model performance for both the multivariate and univariate TSF tasks. Note that a smaller value indicates higher performance for both the MSE and MAE. In the following experimental results, the best results are marked in red and the next best in blue. Avg is the averaged result from all four prediction lengths. All experiments are implemented in PyTorch and conducted on a single NVIDIA RTX3090 24GB GPU.

¹<https://drive.google.com/drive/folders/13Cg1KY01zM5C7K8gK8NfC-F3EYxkM3D2>

5 EXPERIMENTAL RESULTS

The results for multivariate and univariate predictions on time series datasets are summarized in Tables 1, 2 and 3. In general, our model outperforms the selected baselines on both multivariate and univariate forecasting tasks. Detailed results of the experiment can be found in the Appendix A.4.

Multivariate Results For multivariate sequence prediction, as shown in Tables 1 and 2, in general, the WinNet essentially achieves the best performance for the listed datasets on the two measurements. Quantitatively, from the results of the long-input length experiments, WinNet improves 18.5% in MSE and 12.0% in MAE compared to the CNN-based SOTA model TimesNet, indicating that WinNet can more stably capture the long and short periodicity in data. As for the results of the short-input experiments, compared to the CNN-based TimesNet, the WinNet improves 9.3% in MSE and 8.4% in MAE; compared to the MLP-based DLinear, the WinNet improves 11.9% in MSE and 9.6% in MAE. It is noted that our model achieves a complete outperformance on the ETT datasets for both long and short sequences.

Univariate Results The results of univariate prediction is shown in Table 3. The WinNet significantly outperforms other SOTA models on all datasets, achieving a improvement of 8.2% in MSE and 5.0% in MAE for PatchTST, 12.3% in MSE and 8.1% in MAE for TimesNet, 18.9% in MSE and 13.1% in MAE for DLinear. This demonstrates that the modules in WinNet indeed bring more useful periodic information for univariate TSF tasks.

Table 1: Results for multivariate long-input length prediction. The input sequence length is set to 104 for the ILI dataset and 512 for the others. See Appendix Table 16 for the full results.

Methods	WinNet (Ours)	RLinear (2023a)	RMLP (2023a)	PatchTST (2023)	TimesNet (2023)	MICN (2023)	Crossformer (2023)	DLinear (2023)	FEDformer (2022)	Autoformer (2021)
	MSE MAE	MSE MAE	MSE MAE	MSE MAE	MSE MAE	MSE MAE	MSE MAE	MSE MAE	MSE MAE	MSE MAE
ETTM1	0.345 0.371	0.378 0.401	0.367 0.397	0.352 0.382	0.407 0.417	0.372 0.399	0.424 0.438	0.352 0.381	0.382 0.422	0.515 0.493
ETTM2	0.248 0.310	0.281 0.346	0.291 0.350	0.256 0.316	0.283 0.336	0.299 0.357	0.418 0.432	0.267 0.331	0.291 0.343	0.310 0.356
ETTh1	0.402 0.419	0.442 0.456	0.461 0.468	0.418 0.432	0.485 0.481	0.523 0.513	0.440 0.454	0.424 0.438	0.428 0.453	0.473 0.476
ETTh2	0.332 0.385	0.469 0.463	0.425 0.448	0.342 0.385	0.414 0.445	0.668 0.557	0.443 0.455	0.431 0.446	0.387 0.434	0.422 0.442
ILI	1.919 0.912	2.347 1.101	2.350 1.084	1.538 0.841	2.345 1.037	2.526 1.060	3.394 1.215	2.169 1.041	2.596 1.069	2.819 1.119
Exchange	0.401 0.415	0.466 0.451	0.495 0.515	0.392 0.416	0.618 0.557	0.440 0.474	0.798 0.693	0.416 0.430	0.477 0.477	0.613 0.539
Weather	0.219 0.263	0.231 0.294	0.231 0.278	0.229 0.265	0.252 0.287	0.245 0.300	0.227 0.285	0.231 0.280	0.310 0.357	0.335 0.379
Traffic	0.417 0.285	0.419 0.290	0.404 0.280	0.396 0.265	0.616 0.334	0.489 0.300	0.528 0.293	0.433 0.295	0.603 0.372	0.616 0.383
Electricity	0.159 0.253	0.167 0.261	0.162 0.256	0.161 0.253	0.200 0.301	0.188 0.296	0.304 0.355	0.166 0.263	0.207 0.321	0.214 0.326

Table 2: Results for multivariate short-input length prediction. The input sequence length is set to 36 for the ILI dataset and 96 for the others. See Appendix Table 17 for the full results.

Methods	WinNet (Ours)	RLinear (2023a)	RMLP (2023a)	PatchTST (2023)	TimesNet (2023)	MICN (2023)	Crossformer (2023)	DLinear (2023)	FEDformer (2022)	Autoformer (2021)
	MSE MAE	MSE MAE	MSE MAE	MSE MAE	MSE MAE	MSE MAE	MSE MAE	MSE MAE	MSE MAE	MSE MAE
ETTM1	0.381 0.385	0.395 0.404	0.400 0.414	0.382 0.395	0.392 0.413	0.400 0.405	0.470 0.468	0.403 0.406	0.448 0.452	0.587 0.517
ETTM2	0.276 0.320	0.312 0.366	0.330 0.370	0.285 0.330	0.328 0.382	0.291 0.332	0.470 0.468	0.350 0.400	0.304 0.349	0.327 0.370
ETTh1	0.439 0.425	0.466 0.462	0.462 0.454	0.470 0.452	0.558 0.535	0.460 0.455	0.518 0.503	0.455 0.451	0.440 0.459	0.496 0.487
ETTh2	0.375 0.400	0.460 0.459	0.515 0.482	0.384 0.406	0.587 0.525	0.414 0.427	0.491 0.486	0.558 0.515	0.436 0.449	0.449 0.459
ILI	2.388 0.977	3.061 1.202	3.483 1.280	1.833 0.845	2.664 1.085	2.138 0.930	4.251 1.406	2.615 1.090	2.846 1.143	3.006 1.161
Exchange	0.373 0.406	0.339 0.401	0.396 0.432	0.367 0.402	0.334 0.425	0.416 0.443	0.764 0.651	0.354 0.413	0.518 0.499	0.613 0.539
Weather	0.250 0.293	0.267 0.320	0.251 0.295	0.257 0.279	0.242 0.299	0.259 0.286	0.248 0.305	0.265 0.316	0.308 0.360	0.337 0.381
Traffic	0.457 0.356	0.630 0.390	0.546 0.352	0.541 0.348	0.541 0.315	0.619 0.335	0.558 0.309	0.624 0.383	0.609 0.376	0.627 0.378
Electricity	0.192 0.280	0.206 0.298	0.202 0.291	0.211 0.297	0.186 0.294	0.192 0.295	0.320 0.372	0.211 0.300	0.213 0.326	0.227 0.337

Table 3: Results for univariate long-input length prediction. The input sequence length is set to 104 for the ILI dataset and 336 for the others. See Appendix Table 18 for the full results.

Methods	WinNet (Ours)		RLinear (2023a)		RMLP (2023a)		PatchTST (2023)		TimesNet (2023)		MICN (2023)		DLinear (2023)		FEDformer (2022)		Autoformer (2021)	
	MSE	MAE	MSE	MAE	MSE	MAE	MSE	MAE	MSE	MAE	MSE	MAE	MSE	MAE	MSE	MAE	MSE	MAE
ETTh1	0.044	0.157	0.054	0.170	0.074	0.208	0.048	0.162	0.053	0.173	0.049	0.164	0.053	0.167	0.069	0.201	0.080	0.221
ETTm2	0.109	0.246	0.114	0.253	0.133	0.276	0.112	0.251	0.132	0.275	0.111	0.247	0.112	0.247	0.119	0.261	0.129	0.271
ETTh1	0.069	0.207	0.105	0.249	0.123	0.277	0.073	0.210	0.074	0.215	0.102	0.251	0.103	0.246	0.111	0.257	0.104	0.252
ETTh2	0.178	0.334	0.205	0.359	0.222	0.374	0.176	0.336	0.180	0.341	0.190	0.342	0.198	0.350	0.205	0.349	0.217	0.363
Weather	0.0013	0.0280	0.0063	0.0662	0.0041	0.0498	0.0014	0.0282	0.0015	0.0295	0.0064	0.0675	0.0062	0.0665	0.0042	0.0526	0.0063	0.0581
Exchange	0.484	0.472	0.520	0.519	0.574	0.583	0.456	0.508	0.583	0.535	0.534	0.543	0.566	0.544	0.725	0.637	0.789	0.681
ECL	0.258	0.359	0.257	0.359	0.284	0.381	0.400	0.442	0.307	0.394	0.317	0.412	0.257	0.360	0.456	0.507	0.551	0.558
Traffic	0.132	0.217	0.134	0.219	0.148	0.238	0.141	0.223	0.144	0.234	0.152	0.240	0.144	0.238	0.302	0.398	0.263	0.370
ILI	0.665	0.613	1.921	1.223	1.095	0.920	0.794	0.684	0.777	0.723	1.279	0.913	0.714	0.695	1.107	0.922	1.139	0.931

Table 4: Results for ablation studies, including the I2PE, TDPD and DCB in WinNet. Four cases are included: (a) all the three modules are included in model (Final: I2PE+TDPD+DCB); (b) only the TDPD; (c) TDPD+DCB; (d) the original version with common CNN and one-dimensional trend decomposition.

Methods	WinNet								TimesNet*		DLinear		
	Final		TDPD+DCB		TDPD		original		MSE	MAE	MSE	MAE	
Weather	96	0.143	0.198	0.147	0.203	0.147	0.206	0.147	0.208	0.163	0.223	0.176	0.237
	192	0.188	0.240	0.191	0.244	0.191	0.244	0.193	0.253	0.218	0.266	0.192	0.246
	336	0.235	0.280	0.240	0.290	0.245	0.290	0.246	0.300	0.280	0.306	0.240	0.287
	720	0.310	0.336	0.315	0.340	0.321	0.342	0.326	0.357	0.349	0.356	0.316	0.352
ECL	96	0.129	0.225	0.135	0.231	0.139	0.237	0.145	0.249	0.181	0.281	0.140	0.237
	192	0.147	0.240	0.150	0.244	0.153	0.249	0.163	0.266	0.193	0.293	0.153	0.249
	336	0.163	0.257	0.167	0.261	0.169	0.264	0.180	0.283	0.205	0.312	0.169	0.267
	720	0.198	0.290	0.211	0.300	0.208	0.297	0.217	0.315	0.222	0.320	0.203	0.301
traffic	96	0.394	0.274	0.405	0.281	0.414	0.288	0.528	0.300	0.603	0.328	0.410	0.282
	192	0.407	0.279	0.420	0.287	0.428	0.294	0.549	0.312	0.610	0.329	0.423	0.287
	336	0.416	0.283	0.437	0.295	0.442	0.302	0.569	0.323	0.619	0.330	0.436	0.296
	720	0.453	0.305	0.465	0.312	0.468	0.316	0.610	0.340	0.632	0.352	0.466	0.315

* We replace the input length L=512 in TimesNet for a fair comparison.

6 ABLATION STUDIES

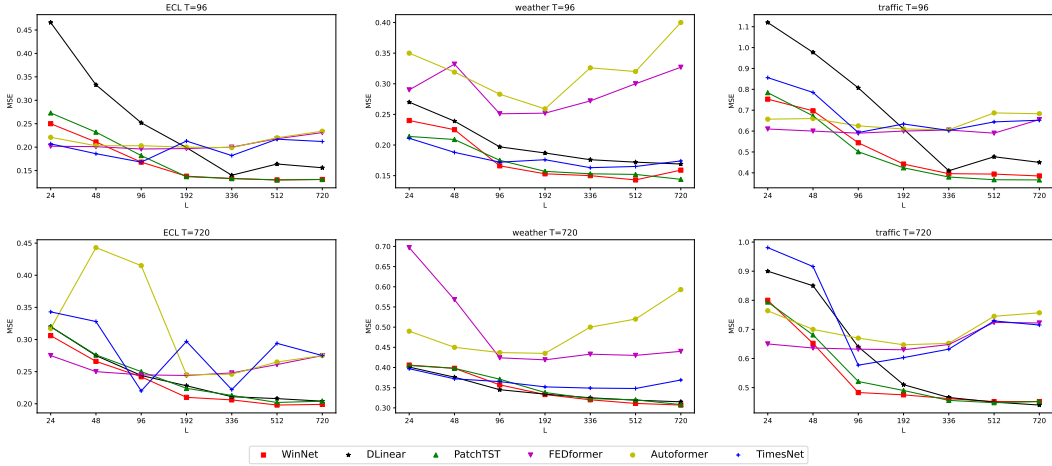
Model architecture To validate the proposed modules in the WinNet, the ablation studies are conducted to determine the best model architecture, including the I2PE, TDPD, and DCB. The TimesNet and DLinear are as a SOTA benchmark for CNN-based and MLP-based models. Based on the results in Table 4, we can see that all the proposed modules can significantly improve the prediction performance, which validates the proposed model architecture. **We also explore the effect of both the intra-period and inter-period on the proposed model performance, as shown in Appendix Table 11 and 12.** Ablation study results on ETT datasets are available in Appendix Table 13.

In the original version, normal trend decomposition and a regular CNN network are applied to replace the I2PE and TDPD, respectively. Compared to using the TDPD, the original version fails to capture the periodicity in complex datasets and suffers from inferior results over the DLinear. Taking the traffic dataset as an example, the TDPD module can improve on the MSE by 22.3%, and achieve comparable results with the DLinear. Other modules can also contribute expected performance improvements and finally outperform the SOTA baselines (TimesNet and DLinear).

Input length In general, we consider that a larger look-back window can capture a long-range of periodicity, such as 96 for DLinear and 512 for PatchTST. To validate this issue, we compare the model performance with input lengths of 96 and 512, and the results are reported in the Table 1

and 2. In addition, other configurations are also considered in the proposed model to validate the performance, including $\{24, 48, 96, 192, 336, 512, 720\}$ as the input length and $\{96, 720\}$ as the prediction length respectively. As can be seen from Figure 5, the predictions of our model are more significant as the prediction length increases.

Figure 5: Prediction error (MSE) with different look-back windows on 3 large datasets: weather, ECL, traffic. The look-back windows are selected to be $L = \{24, 48, 96, 192, 336, 512, 720\}$, and the prediction lengths are $T = \{96, 720\}$.



Model efficiency In addition to the expected performance improvements, we also harvest a higher computational efficiency. Table 5 shows the computational efficiency of our model in the univariate prediction tasks. From the table, we can see that our model can achieve higher efficiency, in terms of computational complexity, number of parameters and memory consumption, even over the simple DLinear model. The efficiency of WinNet on the multi-channel and few-channel datasets can be seen in the Appendix Table 14 and 15.

Table 5: Efficiency of our model on the Traffic dataset vs. other methods in univariate prediction. We set the input length to 720 and the prediction length to 720. See relevant computational efficiency with `top`, `torchsummary` and `torch.cuda.memory_allocated` functions. Times-T denotes the time of an iter training, and Times-I denotes the actual inference time.

Method	WinNet	PatchTST	TimesNet	MICN	Crossformer	DLinear	FEDformer	Autoformer	Informer	Transformer
FLOPs	851.3K	44.2M	3240.7G	5.32G	726.5M	1.04M	1.74G	1.74G	1.41G	1.74G
Params	830.8K	8.69M	450.9M	18.75M	11.09M	1.04M	3.94M	2.37M	2.77M	2.38M
Times-T	17ms	24ms	491ms	25ms	55ms	12ms	430ms	265ms	142ms	45ms
Memory	11MiB	44MiB	1762MiB	85MiB	56MiB	12MiB	24MiB	27MiB	29MiB	27MiB
Times-I	9.6ms	11.2ms	66.9ms	12.7ms	21.2ms	8.6ms	55.0ms	28.2ms	18.1ms	14.1ms

7 CONCLUSIONS

In summary, we propose a CNN-based approach for time series forecasting models by introducing the important modules of periodic window, including the I2PE, TDPD, and DCB. Compared to previous SOTA models, our model captures the correlation between long and short periods and is more effective as the look-back window gets longer. The proposed model not only outperforms other baselines in terms of prediction accuracy, but also harvests higher computational efficiency.

This work demonstrates the potential for the CNN-based methods in the TSF tasks. The correlation between period-trend and oscillation terms can provide the local periodicity in time series. In the future, we should focus on the correlation and interplay between the period-trend and oscillation terms, instead of training them separately.

REFERENCES

- Shaojie Bai, J Zico Kolter, and Vladlen Koltun. An empirical evaluation of generic convolutional and recurrent networks for sequence modeling. *arXiv preprint arXiv:1803.01271*, 2018.
- Junyoung Chung, Caglar Gulcehre, KyungHyun Cho, and Yoshua Bengio. Empirical evaluation of gated recurrent neural networks on sequence modeling. *arXiv:1412.3555v1*, 2014.
- Alexey Dosovitskiy, Lucas Beyer, Alexander Kolesnikov, Dirk Weissenborn, Xiaohua Zhai, Thomas Unterthiner, Mostafa Dehghani, Matthias Minderer, George Heigold, Sylvain Gelly, and et al. An image is worth 16x16 words: Transformers for image recognition at scale. *arXiv preprint arXiv:2010.11929*, 2020.
- Vijay Ekambaram, Arindam Jati, Nam Nguyen, Phanwadee Sinthong, and Jayant Kalagnanam. Tsmixer: Lightweight mlp-mixer model for multivariate time series forecasting. *Proceedings of the 29th ACM SIGKDD Conference on Knowledge Discovery and Data Mining (KDD '23)*, 2023. URL <https://doi.org/10.1145/3580305.3599533>.
- Sepp Hochreiter and Jürgen Schmidhuber. Long short-term memory. *Neural Computation*, 9(8): 1735–1780, 1997. doi: 10.1162/neco.1997.9.8.1735.
- Guokun Lai, Weicheng Chang, Yiming Yang, and Hanxiao Liu. Modeling long-and short-term temporal patterns with deep neural networks. *SIGIR*, 2018.
- Zhe Li, Shiyi Qi, Yiduo Li, and Zenglin Xu. Revisiting long-term time series forecasting: An investigation on linear mapping. *ArXiv*, abs/2305.10721, 2023a.
- Zhe Li, Zhongwen Rao, Lujia Pan, and Zenglin Xu. Mts-mixers: Multivariate time series forecasting via factorized temporal and channel mixing. *ArXiv*, abs/2302.04501, 2023b.
- Shengsheng Lin, Weiwei Lin, Wentai Wu, Songbo Wang, and Yongxiang Wang. Petformer: Long-term time series forecasting via placeholder-enhanced transformer. *arXiv:2308.04791v1*, 2023.
- Yuqi Nie, Nam H Nguyen, Phanwadee Sinthong, and Jayant Kalagnanam. A time series is worth 64 words: Long-term forecasting with transformers. *International Conference on Learning Representations (ICLR)*, 2023.
- David Salinas, Valentin Flunkert, Jan Gasthaus, and Tim Januschowski. Deepar: Probabilistic forecasting with autoregressive recurrent networks. *International Journal of Forecasting*, 2020. URL <https://doi.org/10.48550/arXiv.1704.04110>.
- Christian Szegedy, Wei Liu, Yangqing Jia, Pierre Sermanet, Scott E. Reed, Dragomir Anguelov, D. Erhan, Vincent Vanhoucke, and Andrew Rabinovich. Going deeper with convolutions. *CVPR*, 2015.
- Ashish Vaswani, Noam Shazeer, Niki Parmar, Jakob Uszkoreit, Llion Jones, Aidan N Gomez, Lukasz Kaiser, and Polosukhin Illia. Attention is all you need. *Proceedings of the Advances in Neural Information Processing Systems (NeurIPS)*, 2017.
- Huiqiang Wang, Jian Peng, Feihu Huang, Jince Wang, Junhui Chen, and Yifei Xiao. Micn: Multi-scale local and global context modeling for long-term series forecasting. *ICLR*, 2023.
- Haixu Wu, Jiehui Xu, Jianmin Wang, and Mingsheng Long. Autoformer: Decomposition transformers with auto-correlation for long-term series forecasting. *Advances in Neural Information Processing Systems (NeurIPS)*, 2021.
- Haixu Wu, Tengge Hu, Yong Liu, Hang Zhou, Jianmin Wang, and Mingsheng Long. Timesnet: Temporal 2d-variation modeling for general time series analysis. *International Conference on Learning Representations (ICLR)*, 2023.
- Ailing Zeng, Muxi Chen, Lei Zhang, and Qiang Xu. Are transformers effective for time series forecasting? *Proceedings of the AAAI Conference on Artificial Intelligence (AAAI)*, 2023.

T. Zhang, Yizhuo Zhang, Wei Cao, J. Bian, Xiaohan Yi, Shun Zheng, and Jian Li. Less is more: Fast multivariate time series forecasting with light sampling-oriented mlp structures. *arXiv preprint arXiv:2207.01186*, 2022.

Yunhao Zhang and Junchi Yan. Crossformer: Transformer utilizing cross-dimension dependency for multivariate time series forecasting. *ICLR*, 2023.

Haoyi Zhou, Shanghang Zhang, Jieqi Peng, Shuai Zhang, Jianxin Li, Hui Xiong, and Wancai Zhang. Informer: Beyond efficient transformer for long sequence time-series forecasting. *Proceedings of the AAAI Conference on Artificial Intelligence (AAAI)*, 2021.

Tian Zhou, Ziqing Ma, Qingsong Wen, Xue Wang, Liang Sun, and Rong Jin. Fedformer: Frequency enhanced decomposed transformer for long-term series forecasting. *International Conference on Machine Learning(ICML)*, 2022.

A APPENDIX

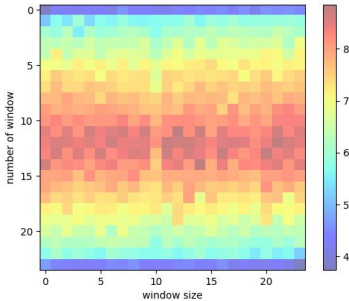
A.1 EXPERIMENT DETAILS

Datasets characteristics The dataset is characterised as follows in Appendix Table 6. We follow standard protocol (Nie et al., 2023) and split all datasets into training, validation and test set in chronological order by the ratio of 6:2:2 for the ETT dataset and 7:1:2 for the other datasets. Frequency indicates the sampling time difference between neighbouring time steps.

Table 6: Summary of experiment datasets.

Datasets	ETTM1	ETTM2	ETTh1	ETTh2	weather	ILI	exchange	traffic	ECL
Channels	7	7	7	7	21	7	7	862	321
Lengths	69680	69680	17420	17420	52696	966	7588	17544	26304
Frequency	15min	15min	1h	1h	10min	7day	1day	1h	1h

Figure 6: The features after the Decomposition Correlation Block. In the figure, the rows represent periodic windows and the columns represent the number of windows.



Decomposition Correlation Block Convolutional networks can extract the local correlation between period-trend and oscillation terms based on the weights of the convolutional kernel. A higher weight means the relatively higher correlation. As shown in Appendix Figure 6, we visualise the heat map after the convolution kernel and can see that the model focuses more on the local periodicity of the intermediate window from 5 to 18 for the 2D tensor. In terms of periods, our model pays more attention to the previous 10-15 periods when forecasting.

Two-Dimensional Period Decomposition We take real data from ETTh1 for TDPD and get the period-trend and oscillation terms. As demonstrated in Appendix Figure 7, each column of the period-trend keeps essentially the same trend. In contrast, the oscillation term is characterised by disorganized distributions.

Figure 7: Showcase of the TDPD.

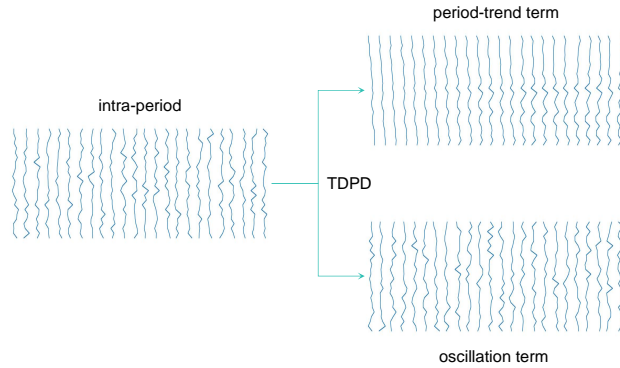
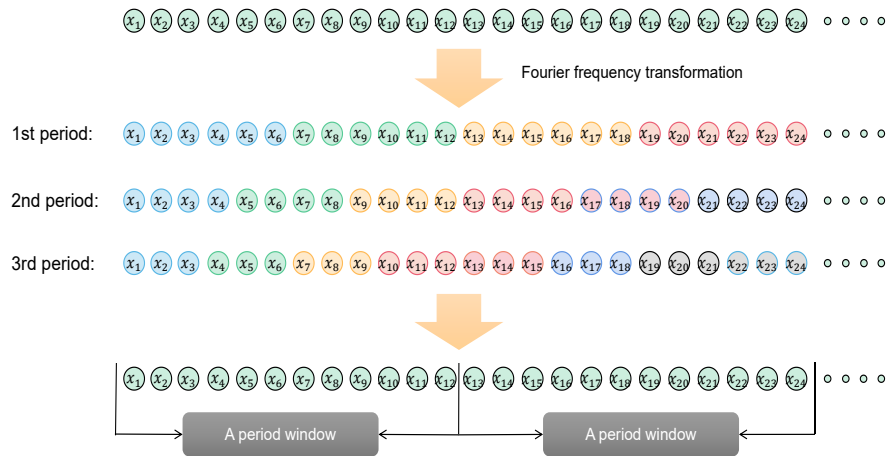


Figure 8: Period Window. The samples with same colour in each row represent time steps in a same period. A sequence can obtain its top-k period values by FFT. The 1st period indicates the most dominant period in the sequence, and so on. For example, the top-3 periods are $\{6, 4, 3\}$ and approximated multiples of these periods are selected as the size of the periodic window, i.e. 12.



A.2 MORE ABLATION STUDIES

Window size As shown in Appendix Figure 8, since the window size is approximated as a multiple of the multi-short periods, it can also have implications for experimental performance of the proposed model. For example, for a sequence with top-4 periods $\{4, 6, 8, 12\}$, we can take 24 as the window size, but it is equally possible to approximate the period of 8 as 9 and take 36 as the final window size. The top-4 periods for the datasets can be seen in Table 8. As demonstrated in Appendix Table 9, the proposed approach can achieve better performance for the periodic window of 24.

Table 7: Period frequencies obtained by FFT for each dataset before MLP. The 1st period represents the period with the highest number of occurrences, and so on. Period represents the specific value of periods and count represents the number of occurrences. It can be seen that most datasets have large periods, difficult to capture the periodicity through CNNs.

topk periods	1st period		2nd period		3rd period		4th period	
	period	count	period	count	period	count	period	count
statistics	168	759	336	759	112	759	67	759
weather	112	711	84	711	336	711	168	711
ETTm1	168	374	336	294	84	235	112	234
ECL	336	711	112	711	84	711	168	711
ETTm2	24	171	336	171	12	171	168	171
ETTh1	24	246	12	246	8	246	168	246
traffic	336	101	168	101	112	101	84	101
exchange	336	171	24	171	168	171	112	171
ETTh2								

Table 8: Period frequencies obtained by FFT for each dataset after MLP. The 1st period represents the period with the highest number of occurrences, and so on. Period represents the specific value of periods and count represents the number of occurrences. 11/12 or 23/24 mean that we use these two periods approximately as one period. Based on these periods, the multiples of them are selected to be the size of the periodic window.

topk periods	1st period		2nd period		3rd period		4th period	
	period	count	period	count	period	count	period	count
statistics	3	1075	2	678	23/24	592	11/12	234
weather	2	2528	3	469	23/24	355	4	104
ETTm1	2	592	17	372	3	315	8	191
ECL	23/24	1185	12	749	288	631	192	351
ETTm2	2	332	3	248	5	98	4	55
ETTh1	2	334	4	328	8	222	3	199
traffic	3	125	2	89	6	55	4	48
exchange	2	369	3	202	4	108	11/12	47
ETTh2								

Table 9: Ablation study with different sizes of the periodic window.

Methods	WinNet						TimesNet	DLinear			
	18		24		32						
Metric	MSE	MAE	MSE	MAE	MSE	MAE	MSE	MAE			
ETTm1	96	0.282	0.336	0.283	0.335	0.279	0.334	0.377	0.397	0.290	0.342
	192	0.319	0.357	0.324	0.360	0.323	0.361	0.389	0.401	0.332	0.369
	336	0.354	0.379	0.357	0.379	0.354	0.382	0.393	0.414	0.366	0.392
	720	0.419	0.412	0.416	0.411	0.408	0.414	0.470	0.458	0.420	0.424
ETTm2	96	0.163	0.252	0.160	0.251	0.162	0.251	0.201	0.280	0.167	0.260
	192	0.216	0.290	0.212	0.287	0.216	0.291	0.242	0.313	0.224	0.303
	336	0.271	0.325	0.261	0.322	0.268	0.323	0.310	0.356	0.281	0.342
	720	0.363	0.385	0.359	0.381	0.360	0.386	0.381	0.396	0.397	0.421
ETTh1	96	0.367	0.392	0.362	0.390	0.374	0.397	0.460	0.464	0.375	0.399
	192	0.402	0.413	0.394	0.410	0.409	0.420	0.458	0.462	0.412	0.420
	336	0.426	0.428	0.419	0.426	0.427	0.430	0.523	0.501	0.439	0.443
	720	0.442	0.454	0.436	0.453	0.434	0.451	0.502	0.497	0.472	0.490
ETTh2	96	0.271	0.333	0.267	0.332	0.275	0.337	0.338	0.397	0.289	0.353
	192	0.326	0.374	0.322	0.372	0.337	0.377	0.422	0.446	0.383	0.418
	336	0.356	0.400	0.351	0.401	0.368	0.414	0.431	0.460	0.448	0.465
	720	0.395	0.437	0.389	0.436	0.406	0.448	0.467	0.480	0.605	0.551
weather	96	0.151	0.207	0.143	0.198	0.146	0.202	0.163	0.223	0.176	0.237
	192	0.196	0.253	0.188	0.240	0.191	0.245	0.218	0.266	0.192	0.246
	336	0.245	0.288	0.235	0.280	0.239	0.289	0.280	0.306	0.240	0.287
	720	0.319	0.341	0.310	0.336	0.315	0.345	0.349	0.356	0.316	0.352
ECL	96	0.141	0.238	0.130	0.226	0.142	0.240	0.181	0.281	0.140	0.237
	192	0.155	0.251	0.147	0.240	0.157	0.253	0.193	0.293	0.153	0.249
	336	0.172	0.268	0.163	0.257	0.174	0.270	0.205	0.312	0.169	0.267
	720	0.211	0.300	0.198	0.290	0.212	0.301	0.222	0.320	0.203	0.301
ILI	24	1.987	0.906	1.985	0.905	2.031	0.934	2.500	1.055	2.215	1.081
	36	1.928	0.915	1.897	0.900	1.889	0.902	2.222	1.007	1.963	0.963
	48	1.904	0.919	1.868	0.910	1.902	0.922	2.304	1.043	2.130	1.024
	60	2.066	0.976	1.928	0.933	2.012	0.958	2.354	1.046	2.368	1.096

* We replace the input length L=512 in TimesNet and MICN for a fair comparison.

CNN Kernel The convolution kernel size determines the receptive field for extracting periodicity from the sequence. In this section, we consider the model performance with different kernel size to $\{3, 5, 7\}$, respectively, and the experimental results are shown in Appendix Table 10. It can be found that a larger convolution kernel causes lower prediction accuracy. The results can be attributed that after the proposed period decomposition, the period of the reshaped sequence is smaller and a larger kernel excessively extracts the temporal correlation from other periods to degrade the model performance, especially in the large datasets, traffic and ECL.

Table 10: Prediction error (MSE & MAE) with different kernel size.

Methods	WinNet						TimesNet*	DLinear			
	3x3		5x5		7x7						
Metric	MSE	MAE	MSE	MAE	MSE	MAE	MSE	MAE			
ETTm1	96	0.283	0.335	0.288	0.339	0.286	0.338	0.377	0.397	0.290	0.342
	192	0.324	0.360	0.335	0.368	0.329	0.364	0.389	0.401	0.332	0.369
	336	0.357	0.379	0.370	0.385	0.366	0.380	0.393	0.414	0.366	0.392
	720	0.416	0.411	0.423	0.414	0.422	0.413	0.470	0.458	0.420	0.424
ETTm2	96	0.160	0.251	0.163	0.252	0.162	0.252	0.201	0.280	0.167	0.260
	192	0.212	0.287	0.216	0.289	0.217	0.290	0.242	0.313	0.224	0.303
	336	0.261	0.322	0.267	0.321	0.269	0.324	0.310	0.356	0.281	0.342
	720	0.359	0.381	0.361	0.382	0.375	0.387	0.381	0.396	0.397	0.421
ETTh1	96	0.362	0.390	0.368	0.392	0.366	0.392	0.460	0.464	0.375	0.399
	192	0.394	0.410	0.410	0.420	0.425	0.434	0.458	0.462	0.412	0.420
	336	0.419	0.426	0.436	0.434	0.442	0.442	0.523	0.501	0.439	0.443
	720	0.436	0.453	0.435	0.453	0.436	0.453	0.502	0.497	0.472	0.490
ETTh2	96	0.267	0.332	0.274	0.337	0.270	0.334	0.338	0.397	0.289	0.353
	192	0.322	0.372	0.337	0.378	0.360	0.399	0.422	0.446	0.383	0.418
	336	0.351	0.401	0.376	0.409	0.364	0.409	0.431	0.460	0.448	0.465
	720	0.389	0.436	0.502	0.532	0.418	0.458	0.467	0.480	0.605	0.551
weather	96	0.143	0.198	0.141	0.239	0.150	0.203	0.163	0.223	0.176	0.237
	192	0.188	0.240	0.193	0.245	0.193	0.244	0.218	0.266	0.192	0.246
	336	0.235	0.280	0.243	0.285	0.244	0.287	0.280	0.306	0.240	0.287
	720	0.310	0.336	0.323	0.346	0.318	0.340	0.349	0.356	0.316	0.352
ECL	96	0.130	0.226	0.141	0.239	0.140	0.238	0.181	0.281	0.140	0.237
	192	0.147	0.240	0.161	0.258	0.161	0.258	0.193	0.293	0.153	0.249
	336	0.163	0.257	0.178	0.274	0.178	0.274	0.205	0.312	0.169	0.267
	720	0.198	0.290	0.212	0.301	0.216	0.306	0.222	0.320	0.203	0.301
traffic	96	0.394	0.274	0.414	0.287	0.415	0.289	0.603	0.328	0.410	0.282
	192	0.407	0.279	0.426	0.294	0.428	0.295	0.610	0.329	0.423	0.287
	336	0.416	0.283	0.436	0.295	0.439	0.297	0.619	0.330	0.436	0.296
	720	0.453	0.305	0.464	0.310	0.467	0.313	0.632	0.352	0.466	0.315
ILI	24	1.985	0.905	2.034	0.923	1.966	0.900	2.500	1.055	2.215	1.081
	36	1.897	0.900	1.906	0.909	1.900	0.902	2.222	1.007	1.963	0.963
	48	1.868	0.910	1.925	0.930	1.906	0.922	2.304	1.043	2.130	1.024
	60	1.928	0.933	1.937	0.934	1.945	0.937	2.354	1.046	2.368	1.096

* We replace the input length $L=512$ in TimesNet for a fair comparison.

Fusion mode In the Series Decoder block, we need to fuse the periodic features extracted by DCB for both intra-period and inter-period. Since they are both square shapes and the inter-period is obtained from the transpose of the intra-period, there are two ways to fuse them: one is to transpose the inter-period back and sum them up, and the other is to sum them up directly. Therefore, we explore the impact of these two fusion modes on the model performance. As shown in Appendix Table 11, we can assume that superior results can be achieved by using direct fusing. Even with the NF approach, WinNet almost outperforms CNN-based TimesNet and MLP-based DLinear.

Intra-Inter period In the WinNet, we get two inputs based on the I2PE block, i.e., intra-period and inter-period. The intra-period represents the local periodicity by rows, while inter-period represents the local periodicity by columns, and a parameter-shared convolutional kernel is utilized to

Table 11: Ablation study the fusion mode of inter-period and intra-period on all datasets in WinNet. NF means the normal fusion, while DF means no transposition, direct fusion.

Methods	WinNet				TimesNet		DLinear		
	DF		NF		MSE	MAE	MSE	MAE	
Metric	MSE	MAE	MSE	MAE	MSE	MAE	MSE	MAE	
ETTm1	96	0.283	0.335	0.286	0.337	0.377	0.397	0.290	0.342
	192	0.324	0.360	0.326	0.360	0.389	0.401	0.332	0.369
	336	0.357	0.379	0.366	0.381	0.393	0.414	0.366	0.392
	720	0.416	0.411	0.421	0.414	0.470	0.458	0.420	0.424
ETTm2	96	0.160	0.251	0.162	0.252	0.201	0.280	0.167	0.260
	192	0.212	0.287	0.217	0.290	0.242	0.313	0.224	0.303
	336	0.261	0.322	0.273	0.326	0.310	0.356	0.281	0.342
	720	0.359	0.381	0.363	0.384	0.381	0.396	0.397	0.421
ETTh1	96	0.362	0.390	0.369	0.393	0.460	0.464	0.375	0.399
	192	0.394	0.410	0.409	0.419	0.458	0.462	0.412	0.420
	336	0.419	0.426	0.432	0.432	0.523	0.501	0.439	0.443
	720	0.436	0.453	0.438	0.456	0.502	0.497	0.472	0.490
ETTh2	96	0.267	0.332	0.270	0.335	0.338	0.397	0.289	0.353
	192	0.322	0.372	0.330	0.376	0.422	0.446	0.383	0.418
	336	0.351	0.401	0.385	0.413	0.431	0.460	0.448	0.465
	720	0.389	0.436	0.424	0.464	0.467	0.480	0.605	0.551
Weather	96	0.143	0.198	0.154	0.206	0.163	0.223	0.176	0.237
	192	0.188	0.240	0.193	0.246	0.218	0.266	0.192	0.246
	336	0.235	0.280	0.244	0.285	0.280	0.306	0.240	0.287
	720	0.310	0.336	0.321	0.342	0.349	0.356	0.316	0.352
ECL	96	0.130	0.226	0.141	0.239	0.181	0.281	0.140	0.237
	192	0.147	0.240	0.156	0.252	0.193	0.293	0.153	0.249
	336	0.163	0.257	0.173	0.269	0.205	0.312	0.169	0.267
	720	0.198	0.290	0.211	0.300	0.222	0.320	0.203	0.301
traffic	96	0.394	0.274	0.414	0.288	0.603	0.328	0.410	0.282
	192	0.407	0.279	0.427	0.294	0.610	0.329	0.423	0.287
	336	0.416	0.283	0.435	0.296	0.619	0.330	0.436	0.296
	720	0.453	0.305	0.465	0.312	0.632	0.352	0.466	0.315
ILI	24	1.985	0.905	2.003	0.923	2.500	1.055	2.215	1.081
	36	1.897	0.900	1.906	0.909	2.222	1.007	1.963	0.963
	48	1.868	0.910	1.925	0.930	2.304	1.043	2.130	1.024
	60	1.928	0.933	1.937	0.934	2.354	1.046	2.368	1.096

* We replace the input length L=512 in TimesNet for a fair comparison.

extract the period variations of each of these two periods. Therefore, we design an ablation study to validate their respective effects on the model prediction ability. From Appendix Table 12, it can be seen that a single period may achieve comparable results against the double period on some datasets, such as weather. However, the single period is less effective on multi-channel large datasets like ECL and traffic.

Table 12: Prediction error (MSE & MAE) with the ablation studies of the inter-intra period. Full means both intra-period and inter-period are used to extract periodic features. Intra means only intra-period inputs are used and inter means only inter-period are used.

Methods		WinNet					
		Inter+Intra		Intra		Inter	
Metric		MSE	MAE	MSE	MAE	MSE	MAE
ETTm1	96	0.283	0.335	0.287	0.338	0.328	0.365
	192	0.324	0.360	0.329	0.361	0.331	0.362
	336	0.357	0.379	0.362	0.380	0.366	0.383
	720	0.416	0.411	0.417	0.410	0.418	0.411
ETTm2	24	0.160	0.251	0.161	0.250	0.164	0.252
	36	0.212	0.287	0.217	0.289	0.219	0.291
	48	0.261	0.322	0.269	0.323	0.275	0.328
	60	0.359	0.381	0.360	0.382	0.360	0.382
ETTh1	96	0.362	0.390	0.378	0.402	0.368	0.396
	192	0.394	0.410	0.412	0.426	0.404	0.420
	336	0.419	0.426	0.436	0.442	0.426	0.434
	720	0.436	0.453	0.451	0.466	0.445	0.461
ETTh2	96	0.267	0.332	0.267	0.333	0.281	0.340
	192	0.322	0.372	0.327	0.376	0.347	0.388
	336	0.351	0.401	0.360	0.404	0.367	0.410
	720	0.389	0.436	0.402	0.440	0.397	0.439
ILI	24	1.985	0.905	2.188	1.008	2.177	1.006
	36	1.897	0.900	1.946	0.917	1.935	0.915
	48	1.868	0.910	1.926	0.932	1.916	0.930
	60	1.928	0.933	1.951	0.943	1.947	0.942
ECL	96	0.130	0.226	0.137	0.235	0.139	0.237
	192	0.147	0.240	0.154	0.251	0.157	0.255
	336	0.163	0.257	0.171	0.268	0.174	0.273
	720	0.198	0.290	0.210	0.300	0.211	0.301
traffic	96	0.394	0.274	0.413	0.301	0.412	0.302
	192	0.407	0.279	0.440	0.322	0.438	0.320
	336	0.416	0.283	0.436	0.311	0.434	0.309
	720	0.453	0.305	0.487	0.345	0.487	0.347
weather	96	0.143	0.198	0.144	0.196	0.152	0.205
	192	0.188	0.240	0.188	0.242	0.193	0.242
	336	0.235	0.280	0.238	0.283	0.244	0.286
	720	0.310	0.336	0.310	0.339	0.312	0.338
Exchange	96	0.085	0.201	0.085	0.202	0.085	0.202
	192	0.180	0.298	0.180	0.300	0.179	0.298
	336	0.307	0.398	0.349	0.421	0.344	0.422
	720	1.032	0.761	1.142	0.782	1.130	0.785

Model architecture We propose three blocks: I2PE, TDPD and DCB. Here, we validate the performance of these 3 modules on the ETT dataset and compare with TimesNet and DLinear.

- original: We process the sequence into the trend-cyclical and seasonal terms by common trend decomposition from DLinear and then extract features by common convolution network, respectively.
- TDPD: We optimise the trend decomposition on the sequence by the TDPD module and also extract features by common convolution network, respectively.
- TDPD+DCB: We utilize the decomposition strategy by the TDPD module and together extract periodic features of the period-trend and oscillation terms by DCB block.
- Final: Unlike the previous ones that used a single input, we design both intra-periodic and inter-periodic inputs into the TDPD and DCB modules, respectively. Combine the extracted features by simply adding them.

Table 13: Ablation study on all ETT datasets of the proposed modules including the I2PE, TDPD and DCB in WinNet. Four cases are included: (a) all the three modules are included in model (Final: I2PE+TDPD+DCB); (b) only the TDPD; (c) TDPD+DCB; (d) the original version with the common CNN and one-dimensional trend decomposition.

Methods	WinNet								TimesNet		DLinear		
	Final	TDPD+DCB	TDPD	original									
Metric	MSE	MAE	MSE	MAE	MSE	MAE	MSE	MAE	MSE	MAE	MSE	MAE	
ETTm1	96	0.284	0.338	0.288	0.341	0.289	0.341	0.292	0.352	0.377	0.397	0.290	0.342
	192	0.326	0.362	0.328	0.363	0.330	0.365	0.327	0.374	0.389	0.401	0.332	0.369
	336	0.359	0.380	0.362	0.385	0.363	0.384	0.357	0.391	0.393	0.414	0.366	0.392
	720	0.420	0.411	0.409	0.413	0.428	0.421	0.409	0.423	0.470	0.458	0.420	0.424
ETTm2	96	0.160	0.251	0.159	0.247	0.161	0.249	0.359	0.390	0.201	0.280	0.167	0.260
	192	0.212	0.287	0.217	0.288	0.217	0.290	0.611	0.511	0.242	0.313	0.224	0.303
	336	0.261	0.322	0.270	0.326	0.268	0.324	0.855	0.613	0.310	0.356	0.281	0.342
	720	0.359	0.381	0.358	0.380	0.359	0.383	1.002	0.674	0.381	0.396	0.397	0.421
ETTth1	96	0.362	0.390	0.363	0.393	0.377	0.404	0.379	0.415	0.460	0.464	0.375	0.399
	192	0.394	0.410	0.397	0.415	0.402	0.418	0.411	0.438	0.458	0.462	0.412	0.420
	336	0.420	0.427	0.422	0.431	0.448	0.450	0.440	0.461	0.523	0.501	0.439	0.443
	720	0.436	0.455	0.437	0.456	0.449	0.461	0.506	0.525	0.502	0.497	0.472	0.490
ETTth2	96	0.267	0.332	0.264	0.332	0.269	0.333	0.842	0.622	0.338	0.397	0.289	0.353
	192	0.322	0.372	0.319	0.372	0.330	0.375	0.971	0.682	0.422	0.446	0.383	0.418
	336	0.351	0.401	0.349	0.401	0.382	0.416	1.098	0.728	0.431	0.460	0.448	0.465
	720	0.389	0.436	0.391	0.437	0.398	0.443	1.428	0.854	0.467	0.480	0.605	0.551

* We replace the input length L=512 in TimesNet for a fair comparison.

Table 14: Efficiency of our model on the ECL dataset vs other methods in multivariate prediction. We set the input length to 720 and the prediction length to 720. See relevant computational efficiency with thop, torchsummary and torch.cuda.memory_allocated functions. Times-T denotes the time of an iter training, and Times-I denotes the inference time. In addition, f. means former.

Method	WinNet	PatchTST	TimesNet	MICN	Crossf.	DLinear	FEDf.	Autof.	Inf.	Transf.
FLOPs	273M	51.1G	1620.1G	5.95G	146.4G	333M	2.35G	2.35G	1.84G	2.17G
Parameter	836.8K	18.18M	226.3M	19.07M	11.1M	1.04M	4.76M	3.19M	3.35M	2.95M
Times-T	0.42s	0.17s	0.70s	0.04s	0.54s	0.01s	0.56s	0.26s	0.14s	0.03s
Memory	12MiB	85MiB	878MiB	88MiB	96MiB	14MiB	39MiB	32MiB	33MiB	31MiB
Times-I	61.3ms	33.3ms	115.1ms	20.2ms	66.8ms	19.9ms	89.4ms	38.9ms	32.3ms	36.5ms

Table 15: Efficiency of our model on the ETTm1 dataset vs. other methods in multivariate prediction. We set the input length to 720 and the prediction length to 720. See relevant computational efficiency with `thop`, `torchsummary` and `torch.cuda.memory_allocated` functions. Times-T denotes the time of an iter training, and Times-I denotes the inference time. In addition, f. means former.

Method	WinNet	PatchTST	TimesNet	MICN	Crossf.	DLinear	FEDf.	Autof.	Inf.	Transf.
FLOPs	5.96M	309M	406.2G	5.33G	3.46G	7.26M	1.75G	1.75G	1.42G	1.75G
Params	830.9K	8.69M	57.28M	18.75M	11.09M	1.04M	3.96M	2.39M	2.78M	2.39M
Times-T	28ms	26ms	500ms	25ms	62ms	15ms	450ms	270ms	150ms	45ms
Memory	11MiB	44MiB	239MiB	85MiB	57MiB	12MiB	24MiB	27MiB	29MiB	27MiB
Times-I	9.8ms	10.6ms	65.2ms	11.6ms	22.0ms	9.1ms	61.4ms	26.5ms	17.4ms	14.2ms

A.3 PREDICTION VISUALIZATION

As shown in Appendix Figure 10, Figure 11, Figure 12, Figure 13, Figure 14, Figure 15, Figure 16, we visualize the long-term univariate prediction results of WinNet from the test set of all eight datasets. Here, we predict {24, 36, 48, 60} steps on ILI dataset and {96, 192, 336, 720} steps on other datasets. It can be seen that the proposed model can achieve the best results. **We also supplement the performance with different look-back windows on ETTs, as shown in Figure 9.**

Figure 9: Prediction error (MSE) with different look-back windows on three ETT datasets: ETTm1, ETTm2, ETTh1. The look-back windows are selected to be $L = \{24, 48, 96, 192, 336, 512, 720\}$, and the prediction lengths are $T = \{96, 720\}$.

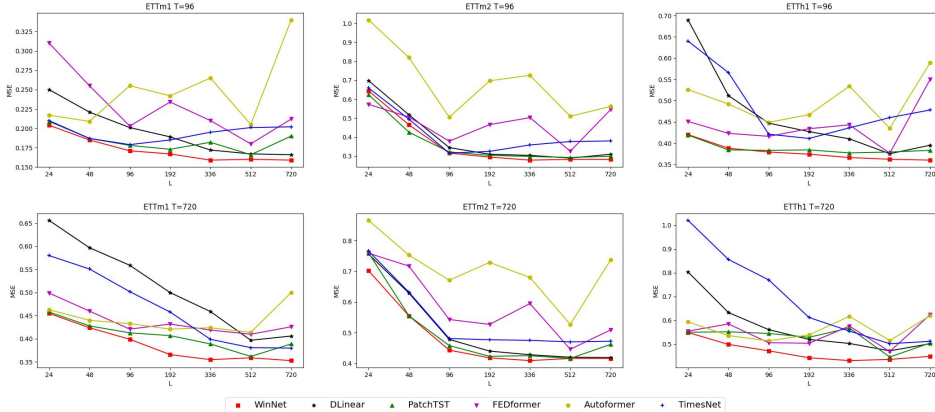


Figure 10: Visualization of prediction on traffic with the look-back window $L=336$.

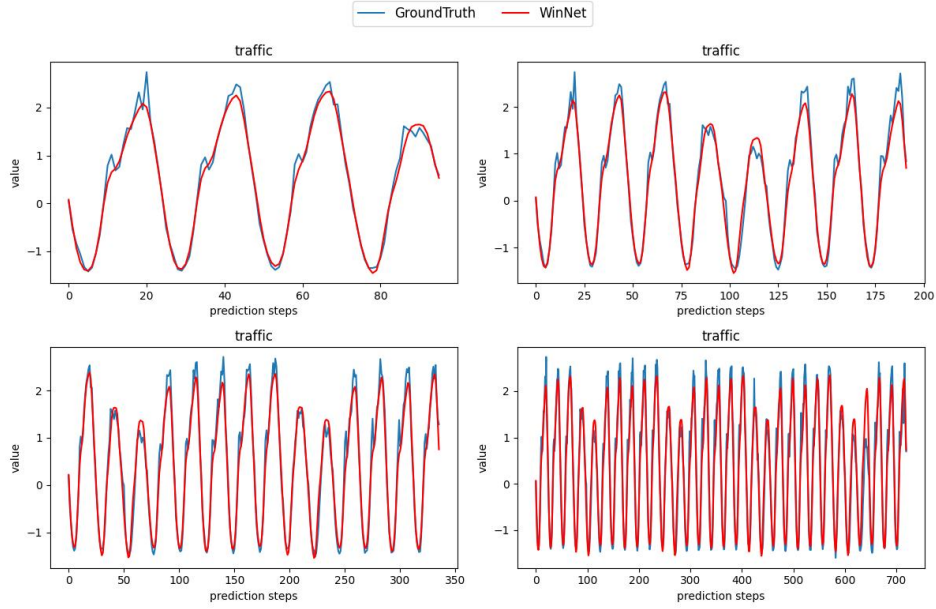


Figure 11: Visualization of prediction on ETTm2 with the look-back window $L=336$.

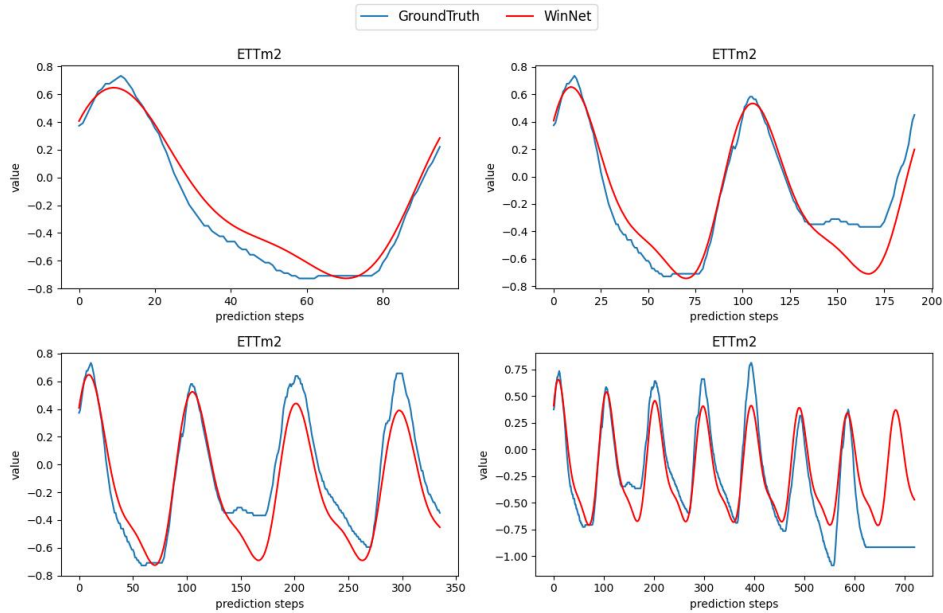


Figure 12: Visualization of prediction on ETTh1 with the look-back window $L=336$.

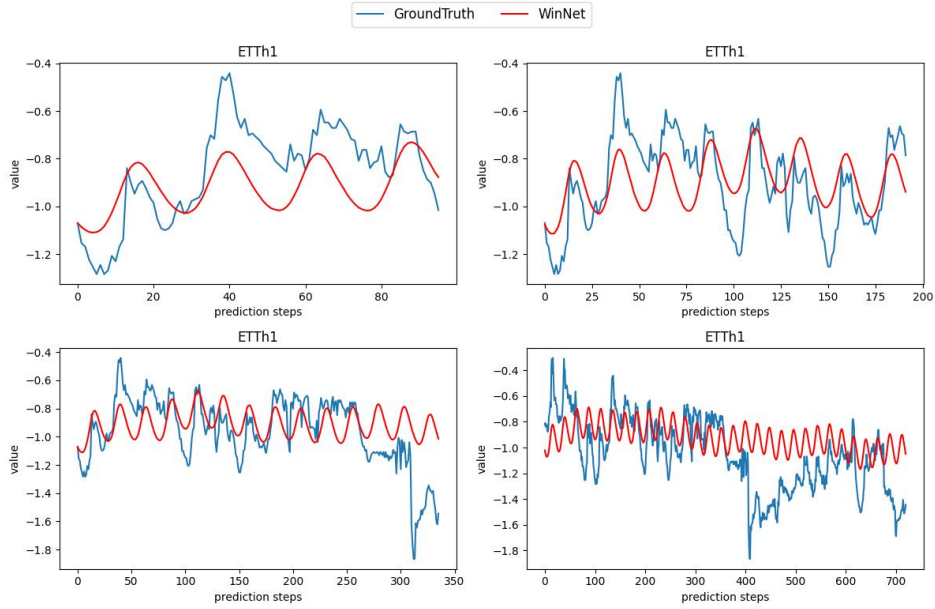


Figure 13: Visualization of prediction on ECL with the look-back window $L=336$.

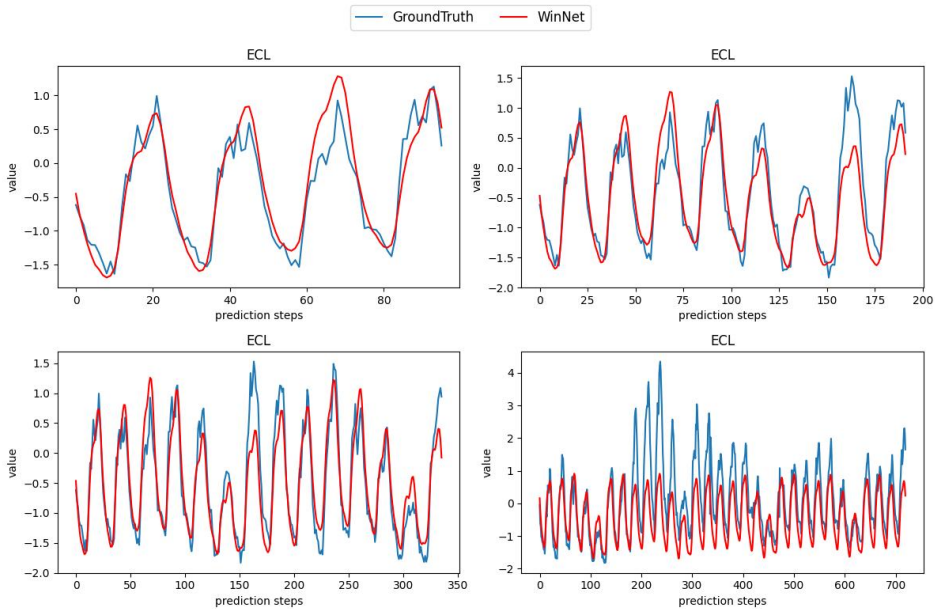


Figure 14: Visualization of prediction on ETTh2 with the look-back window $L=336$.

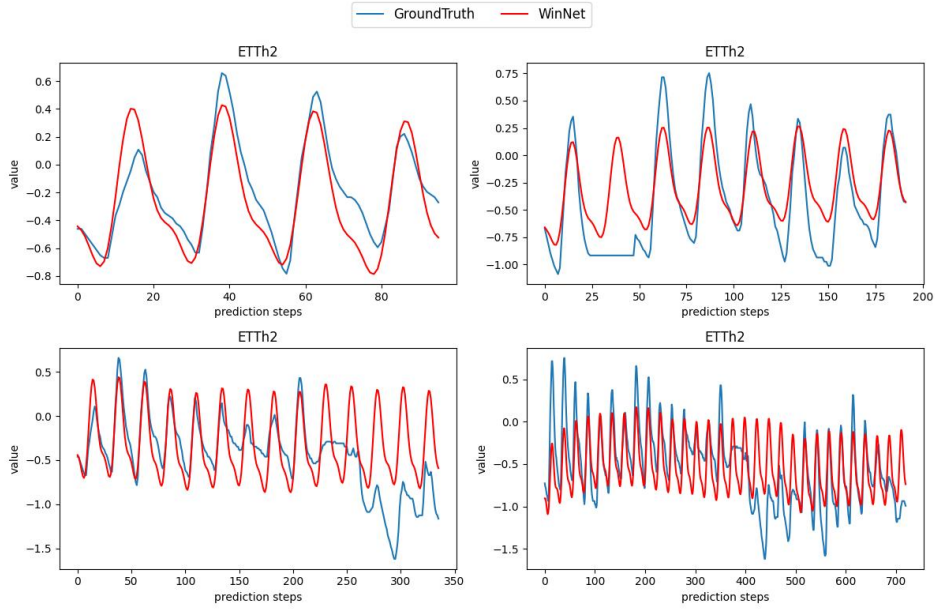


Figure 15: Visualization of prediction on ETTm1 with the look-back window $L=336$.

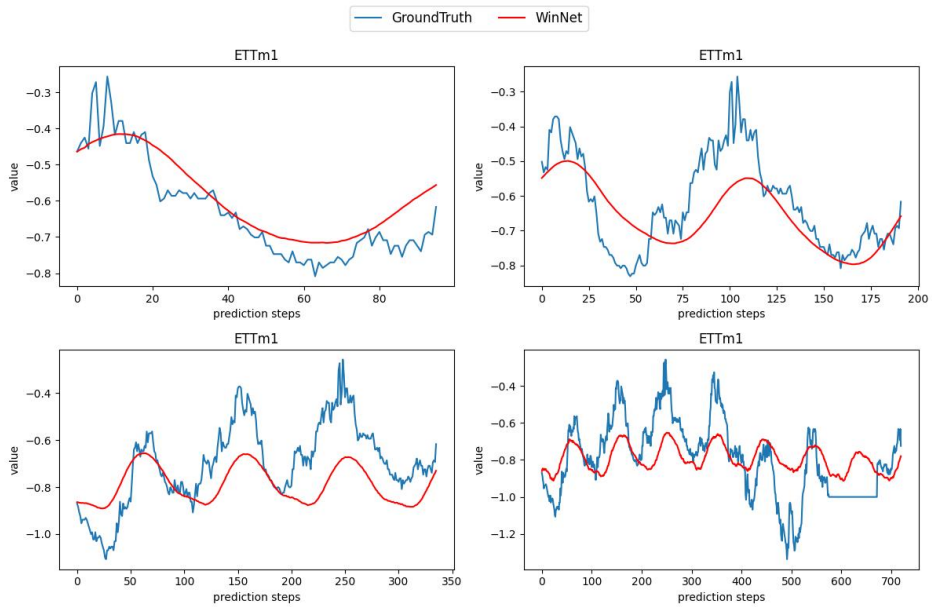
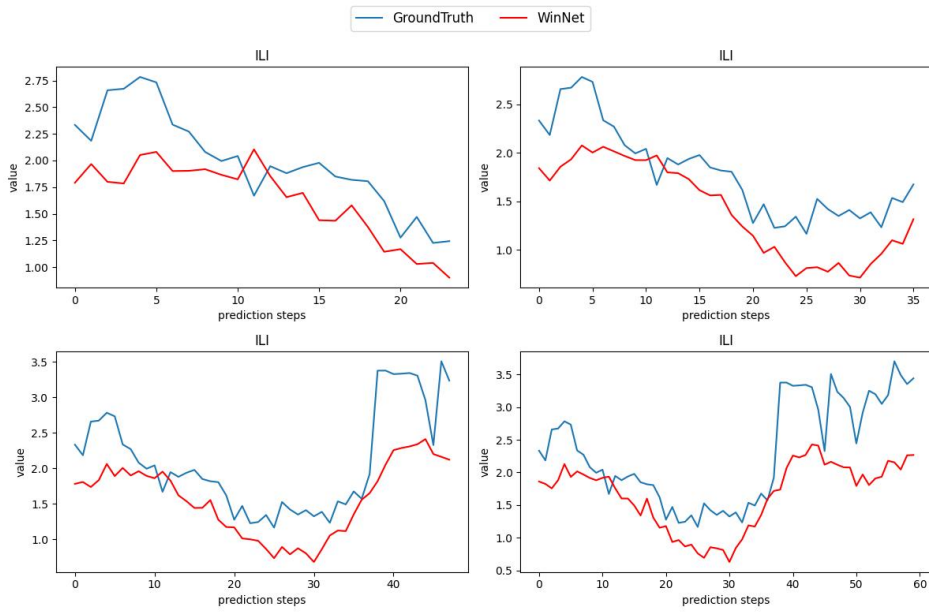


Figure 16: Visualization of prediction on ILI with the look-back window $L=104$.



A.4 FULL RESULTS

Due to the space limitation of the main text, we place the full results of all experiments in the following: multivariate long-input length forecasting in Appendix Table 16, multivariate short-input length forecasting in Appendix Table 17, univariate long-input length forecasting in Appendix Table 18.

Table 16: Full results for multivariate long-input length prediction. We compare extensive competitive models under different prediction lengths. The input sequence length is set to 104 for the ILI dataset and 512 for the others. The 1st count indicates the numbers of best performance.

Methods	WinNet (Ours)	RLinear (2023a)	RMLP (2023a)	PatchTST (2023)	TimesNet (2023)	MICN (2023)	Crossformer (2023)	DLinear (2023)	FEDformer (2022)	Autoformer (2021)	
Metric	MSE MAE	MSE MAE	MSE MAE	MSE MAE	MSE MAE	MSE MAE	MSE MAE	MSE MAE	MSE MAE	MSE MAE	
ETtm1	96	0.283 0.335	0.313 0.358	0.312 0.362	0.293 0.346	0.377 0.397	0.305 0.354	0.302 0.359	0.290 0.342	0.326 0.390	0.510 0.492
	192	0.324 0.360	0.339 0.371	0.344 0.386	0.333 0.370	0.389 0.401	0.362 0.399	0.341 0.387	0.332 0.369	0.365 0.415	0.514 0.495
	336	0.357 0.379	0.441 0.460	0.381 0.409	0.369 0.392	0.393 0.414	0.382 0.405	0.419 0.432	0.366 0.392	0.392 0.425	0.510 0.492
	720	0.416 0.411	0.420 0.418	0.432 0.433	0.416 0.420	0.470 0.458	0.441 0.441	0.637 0.577	0.420 0.424	0.446 0.458	0.527 0.493
	Avg	0.345 0.371	0.378 0.402	0.367 0.398	0.352 0.382	0.407 0.417	0.372 0.399	0.424 0.438	0.352 0.381	0.382 0.422	0.515 0.493
ETtm2	96	0.160 0.251	0.169 0.266	0.184 0.269	0.166 0.256	0.201 0.280	0.189 0.287	0.305 0.361	0.167 0.260	0.180 0.271	0.205 0.293
	192	0.212 0.287	0.258 0.333	0.248 0.325	0.223 0.296	0.242 0.313	0.239 0.323	0.355 0.391	0.224 0.303	0.252 0.318	0.278 0.336
	336	0.261 0.322	0.301 0.358	0.327 0.382	0.274 0.329	0.310 0.356	0.348 0.385	0.420 0.431	0.281 0.342	0.324 0.364	0.343 0.379
	720	0.359 0.381	0.397 0.426	0.406 0.425	0.362 0.385	0.381 0.396	0.421 0.434	0.592 0.548	0.397 0.421	0.410 0.420	0.414 0.419
	Avg	0.248 0.310	0.281 0.346	0.291 0.350	0.256 0.316	0.283 0.336	0.299 0.357	0.418 0.432	0.267 0.331	0.291 0.343	0.310 0.356
ETTh1	96	0.362 0.390	0.371 0.397	0.401 0.430	0.379 0.401	0.460 0.464	0.404 0.429	0.394 0.418	0.375 0.399	0.376 0.415	0.435 0.446
	192	0.394 0.410	0.422 0.439	0.427 0.441	0.413 0.429	0.458 0.462	0.511 0.506	0.423 0.436	0.412 0.420	0.423 0.446	0.456 0.457
	336	0.419 0.426	0.490 0.488	0.469 0.471	0.435 0.436	0.523 0.501	0.482 0.489	0.438 0.451	0.439 0.443	0.444 0.462	0.486 0.487
	720	0.436 0.453	0.484 0.500	0.545 0.528	0.446 0.464	0.502 0.497	0.697 0.631	0.508 0.514	0.472 0.490	0.469 0.492	0.515 0.517
	Avg	0.402 0.419	0.442 0.456	0.461 0.468	0.418 0.432	0.485 0.481	0.523 0.513	0.440 0.454	0.424 0.438	0.428 0.453	0.473 0.476
ETTh2	96	0.267 0.332	0.288 0.355	0.304 0.369	0.274 0.337	0.338 0.397	0.290 0.356	0.395 0.417	0.289 0.353	0.332 0.374	0.332 0.368
	192	0.322 0.372	0.377 0.415	0.381 0.418	0.338 0.376	0.422 0.446	0.415 0.441	0.427 0.438	0.383 0.418	0.407 0.446	0.426 0.434
	336	0.351 0.401	0.426 0.453	0.401 0.440	0.363 0.397	0.431 0.460	0.627 0.573	0.449 0.459	0.448 0.465	0.400 0.447	0.477 0.479
	720	0.389 0.436	0.783 0.627	0.615 0.564	0.393 0.430	0.467 0.480	1.340 0.858	0.501 0.509	0.605 0.551	0.412 0.469	0.453 0.490
	Avg	0.332 0.385	0.469 0.463	0.425 0.448	0.342 0.385	0.414 0.445	0.668 0.557	0.443 0.455	0.431 0.446	0.387 0.434	0.422 0.442
ILI	24	1.985 0.905	2.404 1.142	2.180 1.046	1.522 0.814	2.500 1.055	2.559 1.099	3.383 1.249	2.215 1.081	2.624 1.095	2.906 1.182
	36	1.897 0.900	2.378 1.097	2.272 1.054	1.430 0.834	2.222 1.007	2.483 1.023	3.151 1.157	1.963 0.963	2.516 1.021	2.585 1.038
	48	1.868 0.910	2.478 1.129	2.370 1.084	1.673 0.854	2.304 1.043	2.371 1.007	3.386 1.186	2.130 1.024	2.505 1.041	3.024 1.145
	60	1.928 0.933	2.126 1.035	2.578 1.150	1.529 0.862	2.354 1.046	2.694 1.112	3.658 1.268	2.368 1.096	2.742 1.122	2.761 1.114
	Avg	1.919 0.912	2.347 1.101	2.350 1.084	1.538 0.841	2.345 1.037	2.526 1.060	3.394 1.215	2.169 1.041	2.596 1.069	2.819 1.119
Exchange	96	0.085 0.201	0.086 0.212	0.118 0.256	0.087 0.209	0.160 0.296	0.159 0.312	0.312 0.420	0.086 0.208	0.139 0.276	0.197 0.323
	192	0.180 0.298	0.191 0.325	0.341 0.448	0.190 0.312	0.380 0.451	0.198 0.344	0.589 0.604	0.163 0.299	0.256 0.369	0.300 0.369
	336	0.307 0.398	0.309 0.415	0.727 0.672	0.377 0.446	0.659 0.615	0.323 0.441	0.976 0.817	0.311 0.424	0.426 0.464	0.509 0.524
	720	1.032 0.761	1.277 0.850	0.795 0.685	0.915 0.699	1.276 0.866	1.082 0.800	1.317 0.933	1.107 0.791	1.090 0.800	1.447 0.941
	Avg	0.401 0.415	0.466 0.451	0.495 0.515	0.392 0.416	0.618 0.557	0.440 0.474	0.798 0.693	0.416 0.430	0.477 0.477	0.613 0.539
Weather	96	0.143 0.198	0.159 0.228	0.156 0.212	0.152 0.199	0.163 0.223	0.170 0.235	0.147 0.211	0.176 0.237	0.238 0.314	0.249 0.329
	192	0.188 0.240	0.194 0.264	0.200 0.253	0.197 0.243	0.218 0.266	0.214 0.277	0.194 0.261	0.192 0.246	0.275 0.329	0.325 0.370
	336	0.235 0.280	0.256 0.319	0.253 0.300	0.249 0.283	0.280 0.306	0.278 0.326	0.246 0.306	0.240 0.287	0.339 0.377	0.351 0.391
	720	0.310 0.336	0.315 0.364	0.314 0.346	0.320 0.335	0.349 0.356	0.318 0.363	0.322 0.363	0.316 0.352	0.389 0.409	0.415 0.426
	Avg	0.219 0.263	0.231 0.294	0.231 0.278	0.229 0.265	0.252 0.287	0.245 0.300	0.227 0.285	0.231 0.280	0.310 0.357	0.335 0.379
Traffic	96	0.394 0.274	0.397 0.279	0.377 0.266	0.367 0.251	0.603 0.328	0.461 0.290	0.489 0.276	0.410 0.282	0.576 0.359	0.597 0.371
	192	0.407 0.279	0.407 0.282	0.393 0.275	0.385 0.259	0.610 0.329	0.482 0.302	0.503 0.281	0.423 0.287	0.610 0.380	0.607 0.382
	336	0.416 0.283	0.417 0.289	0.403 0.280	0.398 0.265	0.619 0.330	0.487 0.300	0.528 0.292	0.436 0.296	0.608 0.375	0.623 0.387
	720	0.453 0.305	0.455 0.311	0.441 0.300	0.434 0.287	0.632 0.352	0.527 0.310	0.593 0.326	0.466 0.315	0.621 0.375	0.639 0.395
	Avg	0.417 0.285	0.419 0.290	0.404 0.280	0.396 0.265	0.616 0.334	0.489 0.300	0.528 0.293	0.433 0.295	0.603 0.372	0.616 0.383
Electricity	96	0.130 0.226	0.140 0.235	0.133 0.232	0.130 0.222	0.181 0.281	0.162 0.272	0.198 0.292	0.140 0.237	0.186 0.302	0.196 0.313
	192	0.147 0.240	0.148 0.246	0.147 0.240	0.148 0.240	0.193 0.293	0.176 0.285	0.266 0.330	0.153 0.249	0.197 0.311	0.211 0.324
	336	0.163 0.257	0.171 0.264	0.164 0.261	0.167 0.261	0.205 0.312	0.194 0.301	0.353 0.384	0.169 0.267	0.213 0.328	0.214 0.327
	720	0.198 0.290	0.209 0.297	0.203 0.291	0.202 0.291	0.222 0.320	0.222 0.327	0.400 0.416	0.203 0.301	0.233 0.344	0.236 0.342
	Avg	0.159 0.253	0.167 0.261	0.162 0.256	0.161 0.253	0.200 0.301	0.188 0.296	0.304 0.355	0.166 0.263	0.207 0.321	0.214 0.326
1st count	61	0	4	31	0	0	0	1	0	0	

* We replace the input length L=512 in TimesNet and MICN for a fair comparison. Other experimental results are taken from the PatchTST.

Table 17: All results for multivariate short-input length prediction. The input sequence length is set to 36 for the ILI dataset and 96 for the others. The 1st count indicates the numbers of best performance.

Methods	Metric	WinNet (Ours)	RLinear (2023a)	RMLP (2023a)	PatchTST (2023)	TimesNet (2023)	MICN (2023)	Crossformer (2023)	DLinear (2023)	FEDformer (2022)	Autoformer (2021)
		MSE MAE	MSE MAE	MSE MAE	MSE MAE	MSE MAE	MSE MAE	MSE MAE	MSE MAE	MSE MAE	MSE MAE
ETTm1	96	0.316 0.356	0.338 0.373	0.342 0.377	0.320 0.359	0.316 0.362	0.338 0.375	0.355 0.391	0.345 0.372	0.379 0.419	0.505 0.475
	192	0.368 0.383	0.379 0.395	0.382 0.399	0.364 0.381	0.363 0.390	0.374 0.387	0.416 0.433	0.380 0.389	0.426 0.441	0.553 0.496
	336	0.398 0.402	0.403 0.407	0.404 0.416	0.391 0.401	0.408 0.426	0.410 0.411	0.486 0.479	0.413 0.413	0.445 0.459	0.621 0.537
	720	0.443 0.431	0.461 0.440	0.473 0.462	0.455 0.439	0.481 0.476	0.478 0.450	0.624 0.570	0.474 0.453	0.543 0.490	0.671 0.561
	Avg	0.381 0.385	0.395 0.404	0.400 0.414	0.382 0.395	0.392 0.413	0.400 0.405	0.470 0.468	0.403 0.406	0.448 0.452	0.587 0.517
ETTm2	96	0.171 0.252	0.188 0.281	0.185 0.273	0.181 0.265	0.179 0.275	0.187 0.267	0.356 0.388	0.193 0.292	0.203 0.287	0.255 0.339
	192	0.240 0.300	0.288 0.361	0.252 0.321	0.247 0.307	0.307 0.376	0.249 0.309	0.422 0.440	0.284 0.362	0.269 0.328	0.281 0.340
	336	0.295 0.336	0.326 0.368	0.402 0.416	0.308 0.348	0.325 0.388	0.321 0.351	0.507 0.494	0.369 0.427	0.325 0.366	0.339 0.372
	720	0.399 0.395	0.445 0.452	0.479 0.470	0.406 0.401	0.502 0.490	0.408 0.403	0.598 0.552	0.554 0.522	0.421 0.415	0.433 0.432
	Avg	0.276 0.320	0.312 0.366	0.330 0.370	0.285 0.330	0.328 0.382	0.291 0.332	0.470 0.468	0.350 0.400	0.304 0.349	0.327 0.370
ETTh1	96	0.379 0.388	0.398 0.416	0.378 0.396	0.392 0.408	0.421 0.431	0.389 0.412	0.409 0.432	0.386 0.400	0.376 0.419	0.449 0.459
	192	0.432 0.418	0.450 0.445	0.433 0.432	0.450 0.433	0.474 0.487	0.442 0.442	0.458 0.459	0.437 0.432	0.420 0.448	0.500 0.482
	336	0.474 0.439	0.484 0.463	0.495 0.471	0.518 0.477	0.569 0.551	0.491 0.469	0.509 0.492	0.481 0.459	0.459 0.465	0.521 0.496
	720	0.472 0.457	0.531 0.524	0.540 0.517	0.522 0.490	0.770 0.672	0.521 0.500	0.696 0.632	0.519 0.516	0.506 0.507	0.514 0.512
	Avg	0.439 0.425	0.466 0.462	0.462 0.454	0.470 0.452	0.558 0.535	0.460 0.455	0.518 0.503	0.455 0.451	0.440 0.459	0.496 0.487
ETTh2	96	0.289 0.337	0.300 0.358	0.314 0.374	0.297 0.347	0.299 0.364	0.340 0.374	0.402 0.425	0.333 0.387	0.358 0.397	0.346 0.388
	192	0.375 0.391	0.409 0.428	0.425 0.437	0.390 0.403	0.441 0.454	0.402 0.414	0.452 0.456	0.477 0.476	0.429 0.439	0.456 0.452
	336	0.416 0.428	0.489 0.482	0.480 0.472	0.417 0.429	0.654 0.567	0.452 0.452	0.533 0.506	0.594 0.541	0.496 0.487	0.482 0.486
	720	0.423 0.445	0.641 0.566	0.839 0.645	0.432 0.448	0.956 0.716	0.462 0.468	0.577 0.557	0.831 0.657	0.463 0.474	0.515 0.511
	Avg	0.375 0.400	0.460 0.459	0.515 0.482	0.384 0.406	0.587 0.525	0.414 0.427	0.491 0.486	0.558 0.515	0.436 0.449	0.449 0.459
ILI	24	2.445 0.963	3.044 1.224	3.130 1.200	1.743 0.814	2.684 1.112	2.317 0.934	4.721 1.524	2.398 1.040	3.228 1.260	3.483 1.287
	36	2.465 1.008	3.042 1.178	3.568 1.291	1.579 0.804	2.667 1.068	1.972 0.920	4.148 1.379	2.646 1.088	2.679 1.080	3.103 1.148
	48	2.296 0.961	2.974 1.174	3.529 1.290	2.199 0.897	2.558 1.052	2.238 0.940	4.023 1.354	2.614 1.086	2.622 1.078	2.669 1.085
	60	2.348 0.977	3.184 1.232	3.706 1.338	1.813 0.868	2.747 1.110	2.027 0.928	4.114 1.369	2.804 1.146	2.857 1.157	2.770 1.125
	Avg	2.388 0.977	3.061 1.202	3.483 1.280	1.833 0.845	2.664 1.085	2.138 0.930	4.251 1.406	2.615 1.090	2.846 1.143	3.006 1.161
exchange	96	0.082 0.198	0.083 0.210	0.093 0.229	0.082 0.198	0.099 0.240	0.107 0.234	0.253 0.364	0.088 0.218	0.148 0.278	0.197 0.323
	192	0.173 0.294	0.158 0.294	0.184 0.317	0.173 0.295	0.198 0.354	0.226 0.344	0.482 0.517	0.176 0.315	0.271 0.380	0.300 0.369
	336	0.327 0.412	0.292 0.414	0.385 0.457	0.333 0.415	0.302 0.447	0.367 0.448	0.908 0.748	0.313 0.427	0.460 0.500	0.509 0.524
	720	0.911 0.722	0.824 0.684	0.922 0.723	0.880 0.700	0.738 0.662	0.964 0.746	1.414 0.975	0.839 0.695	1.195 0.841	1.447 0.941
	Avg	0.373 0.406	0.339 0.401	0.396 0.432	0.367 0.402	0.334 0.425	0.416 0.443	0.764 0.651	0.354 0.413	0.518 0.499	0.613 0.539
Weather	96	0.164 0.223	0.198 0.262	0.179 0.234	0.177 0.218	0.161 0.229	0.172 0.220	0.162 0.231	0.196 0.255	0.217 0.296	0.266 0.336
	192	0.213 0.268	0.237 0.295	0.217 0.268	0.225 0.259	0.220 0.281	0.219 0.261	0.211 0.281	0.237 0.296	0.276 0.336	0.307 0.367
	336	0.271 0.313	0.285 0.337	0.265 0.306	0.275 0.296	0.278 0.331	0.280 0.306	0.270 0.328	0.283 0.335	0.339 0.380	0.359 0.395
	720	0.354 0.370	0.346 0.385	0.341 0.372	0.351 0.346	0.311 0.356	0.365 0.359	0.352 0.382	0.345 0.381	0.403 0.428	0.419 0.428
	Avg	0.250 0.293	0.267 0.320	0.251 0.295	0.257 0.279	0.242 0.299	0.259 0.286	0.248 0.305	0.265 0.316	0.308 0.360	0.337 0.381
Traffic	96	0.421 0.344	0.657 0.403	0.540 0.351	0.540 0.357	0.519 0.309	0.593 0.321	0.512 0.288	0.650 0.396	0.587 0.366	0.613 0.388
	192	0.452 0.350	0.603 0.377	0.526 0.344	0.536 0.352	0.537 0.315	0.617 0.336	0.538 0.297	0.598 0.370	0.604 0.373	0.616 0.382
	336	0.475 0.362	0.610 0.380	0.539 0.347	0.547 0.355	0.534 0.313	0.629 0.336	0.569 0.315	0.605 0.373	0.621 0.383	0.622 0.337
	720	0.483 0.371	0.651 0.401	0.577 0.366	0.541 0.330	0.577 0.325	0.640 0.350	0.613 0.336	0.645 0.394	0.626 0.382	0.660 0.408
	Avg	0.457 0.356	0.630 0.390	0.546 0.352	0.541 0.348	0.541 0.315	0.619 0.335	0.558 0.309	0.624 0.383	0.609 0.376	0.627 0.378
Electricity	96	0.167 0.259	0.199 0.286	0.184 0.271	0.208 0.297	0.164 0.269	0.168 0.272	0.224 0.310	0.197 0.282	0.193 0.308	0.201 0.317
	192	0.177 0.265	0.187 0.281	0.187 0.276	0.198 0.288	0.177 0.285	0.184 0.289	0.281 0.345	0.196 0.285	0.201 0.315	0.222 0.334
	336	0.193 0.282	0.200 0.295	0.201 0.292	0.200 0.285	0.193 0.304	0.198 0.300	0.351 0.394	0.209 0.301	0.214 0.329	0.231 0.338
	720	0.232 0.317	0.236 0.328	0.236 0.324	0.241 0.318	0.212 0.321	0.220 0.320	0.426 0.439	0.245 0.333	0.246 0.355	0.254 0.361
	Avg	0.192 0.280	0.206 0.298	0.202 0.291	0.211 0.297	0.186 0.294	0.192 0.295	0.320 0.372	0.211 0.300	0.213 0.326	0.227 0.337
1st count		51	4	0	19	15	0	3	0	3	0

* We replace the input length L=96 in PatchTST and Crossformer for a fair comparison. Other experimental results are taken from the TimesNet and PETformer.

Table 18: All results for univariate long-input length prediction. The input sequence length is set to 104 for the ILL dataset and 336 for the others. The 1st count indicates the numbers of the performance.

Methods		WinNet (Ours)		RLinear (2023a)		RMLP (2023a)		PatchTST (2023)		TimesNet (2023)		MICN (2023)		DLinear (2023)		FEDformer (2022)		Autoformer (2021)	
Metric		MSE	MAE	MSE	MAE	MSE	MAE	MSE	MAE	MSE	MAE	MSE	MAE	MSE	MAE	MSE	MAE	MSE	MAE
ETTh1	96	0.025	0.120	0.029	0.127	0.053	0.179	0.026	0.121	0.028	0.126	0.027	0.123	0.028	0.123	0.033	0.140	0.056	0.183
	192	0.038	0.148	0.043	0.154	0.052	0.174	0.039	0.150	0.048	0.167	0.043	0.154	0.045	0.156	0.058	0.186	0.081	0.216
	336	0.051	0.171	0.064	0.187	0.111	0.265	0.053	0.173	0.060	0.188	0.052	0.173	0.061	0.182	0.084	0.231	0.076	0.218
	720	0.062	0.189	0.081	0.212	0.079	0.213	0.074	0.207	0.076	0.213	0.075	0.206	0.080	0.210	0.102	0.250	0.110	0.267
	Avg	0.044	0.157	0.054	0.170	0.073	0.207	0.048	0.162	0.053	0.173	0.049	0.164	0.053	0.167	0.069	0.201	0.080	0.221
ETTh2	96	0.062	0.181	0.067	0.193	0.070	0.197	0.065	0.186	0.076	0.206	0.063	0.183	0.063	0.183	0.067	0.198	0.065	0.189
	192	0.090	0.224	0.095	0.233	0.098	0.239	0.094	0.231	0.107	0.251	0.091	0.225	0.092	0.227	0.102	0.245	0.118	0.256
	336	0.116	0.258	0.122	0.266	0.159	0.313	0.120	0.265	0.135	0.284	0.121	0.265	0.119	0.261	0.130	0.279	0.154	0.305
	720	0.168	0.318	0.173	0.320	0.203	0.353	0.171	0.322	0.210	0.362	0.172	0.317	0.175	0.320	0.178	0.325	0.182	0.335
	Avg	0.109	0.246	0.114	0.253	0.132	0.275	0.112	0.251	0.132	0.275	0.111	0.247	0.112	0.247	0.119	0.261	0.129	0.271
ETTh1	96	0.052	0.176	0.059	0.183	0.078	0.221	0.055	0.179	0.062	0.195	0.059	0.190	0.056	0.180	0.079	0.215	0.071	0.206
	192	0.068	0.203	0.078	0.212	0.094	0.241	0.071	0.205	0.080	0.225	0.087	0.235	0.071	0.204	0.104	0.245	0.114	0.262
	336	0.080	0.225	0.100	0.248	0.116	0.270	0.081	0.225	0.075	0.215	0.089	0.237	0.098	0.244	0.119	0.270	0.107	0.258
	720	0.079	0.225	0.181	0.351	0.205	0.375	0.087	0.232	0.079	0.225	0.176	0.343	0.189	0.359	0.142	0.299	0.126	0.283
	Avg	0.069	0.207	0.105	0.249	0.123	0.276	0.073	0.210	0.074	0.215	0.102	0.251	0.103	0.246	0.111	0.257	0.104	0.252
ETTh2	96	0.128	0.277	0.136	0.287	0.140	0.293	0.129	0.282	0.151	0.310	0.128	0.271	0.131	0.279	0.128	0.271	0.153	0.306
	192	0.168	0.324	0.178	0.333	0.191	0.349	0.168	0.328	0.179	0.337	0.175	0.328	0.176	0.329	0.185	0.330	0.204	0.351
	336	0.194	0.355	0.213	0.372	0.244	0.397	0.185	0.351	0.195	0.356	0.192	0.354	0.209	0.367	0.231	0.378	0.246	0.389
	720	0.222	0.380	0.293	0.442	0.314	0.458	0.224	0.383	0.195	0.363	0.268	0.418	0.276	0.426	0.278	0.420	0.268	0.409
	Avg	0.178	0.334	0.205	0.358	0.222	0.374	0.176	0.336	0.180	0.341	0.190	0.342	0.198	0.350	0.205	0.349	0.217	0.363
Weather	96	0.0010	0.0237	0.0055	0.0604	0.0028	0.0416	0.0012	0.0256	0.0012	0.0257	0.0059	0.0645	0.0055	0.0617	0.0042	0.0533	0.0034	0.0467
	192	0.0012	0.0269	0.0061	0.0656	0.0047	0.0535	0.0013	0.0268	0.0013	0.0281	0.0063	0.0674	0.0061	0.0659	0.0067	0.0669	0.0039	0.0482
	336	0.0014	0.0284	0.0065	0.0680	0.0046	0.0530	0.0014	0.0283	0.0015	0.0298	0.0075	0.0748	0.0064	0.0678	0.0024	0.0394	0.0077	0.0633
	720	0.0019	0.0333	0.0069	0.0706	0.0043	0.0509	0.0019	0.0324	0.0020	0.0345	0.0059	0.0634	0.0068	0.0706	0.0038	0.0510	0.0103	0.0743
	Avg	0.0013	0.0280	0.0063	0.0662	0.0041	0.0498	0.0014	0.0282	0.0015	0.0295	0.0064	0.0675	0.0062	0.0665	0.0042	0.0526	0.0063	0.0581
exchange	96	0.098	0.232	0.125	0.271	0.181	0.332	0.162	0.314	0.156	0.293	0.150	0.328	0.111	0.262	0.369	0.475	0.418	0.516
	192	0.210	0.341	0.235	0.391	0.428	0.518	0.273	0.411	0.264	0.375	0.211	0.377	0.229	0.391	0.511	0.551	0.538	0.591
	336	0.412	0.480	0.395	0.499	0.628	0.632	0.479	0.538	0.501	0.536	0.440	0.524	0.427	0.514	0.713	0.635	0.978	0.760
	720	1.218	0.836	1.324	0.914	1.060	0.850	0.912	0.770	1.411	0.937	1.337	0.943	1.500	1.009	1.307	0.888	1.223	0.857
	Avg	0.484	0.472	0.520	0.519	0.574	0.583	0.456	0.508	0.583	0.535	0.534	0.543	0.566	0.544	0.725	0.637	0.789	0.681
ECL	96	0.202	0.314	0.207	0.319	0.222	0.331	0.247	0.348	0.227	0.338	0.244	0.355	0.208	0.321	0.396	0.471	0.482	0.519
	192	0.239	0.341	0.239	0.340	0.261	0.362	0.315	0.389	0.286	0.382	0.295	0.395	0.238	0.342	0.376	0.460	0.574	0.568
	336	0.276	0.369	0.269	0.365	0.297	0.388	0.490	0.494	0.326	0.401	0.333	0.428	0.273	0.369	0.522	0.543	0.587	0.581
	720	0.317	0.413	0.313	0.414	0.355	0.443	0.550	0.540	0.392	0.455	0.397	0.472	0.310	0.411	0.531	0.555	0.564	0.567
	Avg	0.258	0.359	0.257	0.359	0.283	0.381	0.400	0.442	0.307	0.394	0.317	0.412	0.257	0.360	0.456	0.507	0.551	0.558
traffic	96	0.126	0.207	0.128	0.209	0.136	0.218	0.134	0.211	0.144	0.232	0.150	0.249	0.139	0.230	0.250	0.355	0.280	0.388
	192	0.131	0.214	0.131	0.214	0.138	0.223	0.139	0.219	0.142	0.228	0.146	0.225	0.140	0.232	0.216	0.325	0.292	0.398
	336	0.129	0.217	0.131	0.217	0.141	0.233	0.138	0.221	0.139	0.229	0.152	0.239	0.142	0.236	0.331	0.428	0.241	0.354
	720	0.143	0.233	0.145	0.235	0.175	0.276	0.154	0.244	0.153	0.250	0.161	0.249	0.157	0.254	0.414	0.487	0.240	0.341
	Avg	0.132	0.217	0.133	0.218	0.148	0.237	0.141	0.223	0.144	0.234	0.152	0.240	0.144	0.238	0.302	0.398	0.263	0.370
ILL	24	0.619	0.557	1.694	1.135	1.020	0.878	0.845	0.651	0.698	0.661	2.356	1.209	0.742	0.661	1.024	0.880	0.928	0.834
	36	0.677	0.602	1.804	1.183	1.035	0.896	0.698	0.624	0.708	0.680	0.646	0.616	0.553	0.613	1.009	0.897	0.942	0.838
	48	0.683	0.633	2.030	1.265	1.114	0.929	0.806	0.711	0.792	0.740	0.955	0.859	0.700	0.706	1.014	0.886	1.032	0.881
	60	0.683	0.663	2.156	1.308	1.209	0.977	0.827	0.753	0.911	0.814	1.162	0.970	0.863	0.801	1.384	1.025	1.657	1.171
	Avg	0.665	0.613	1.921	1.222	1.095	0.920	0.794	0.684	0.777	0.723	1.279	0.913	0.714	0.695	1.107	0.922	1.139	0.931
1st Count	67		9		0		13		6		0		5		2		0		

* We replace the input length L=336 in TimesNet and MICN for a fair comparison. Other experimental results are taken from the PatchTST.